



# Global parameter sensitivity analysis of modelling water, energy and carbon dynamics in a temperate swamp

Oluwabamise L. Afolabi<sup>1</sup>, Hongxing He<sup>2</sup>, Maria Strack<sup>1</sup>

<sup>1</sup>Department of Geography and Environmental Management, University of Waterloo, Waterloo, N2L 3G1, Canada <sup>2</sup>Great Lakes Forestry Centre, Natural Resources Canada (NRCan), Ottawa, P6A 2E5, Canada

Correspondence to: Oluwabamise L. Afolabi (o4afolabi@uwaterloo.ca)

Abstract. Forested peatlands cover a land area of  $7 \times 10^5$  km² and store  $\sim 77\,\mathrm{Pg}$  C in Canada. However, the carbon (C) cycling of forested peatlands, particularly swamps, has been understudied. Few modelling studies have been done on temperate swamp C cycle partly because of the scarcity of field measurements in this ecosystem. These gaps create uncertainties in modelling the C dynamics of temperate swamps and consequently limit our understanding of this ecosystem. To improve our understanding of the processes, interactions and feedbacks that mediate temperate swamp C cycling, we simulated the long-term (40 years) plant processes, energy, water and C fluxes of Beverly Swamp, a well-preserved swamp in Southern Ontario using a process-based model (CoupModel). CoupModel v6 was systematically calibrated for Beverly Swamp using the Generalized Likelihood Uncertainty Estimate (GLUE) method and validated with field measurements. The GLUE approach and its multicriteria constraints reduced the uncertainties associated with the modelling process and reasonably improved some of the simulation outcomes when compared to the initial single run and prior uniform distribution. Global sensitivity analysis of the parameters identified the important parameters that greatly influence temperate swamp C flux simulations and the interconnections that exist between simulated variables and parameters. Plant-related processes and hydrological variables exerted the strongest control on soil respiration simulation. However, these dynamics may be altered as climate continues to warm in coming decades. Results from this study provide valuable knowledge for predicting the fate of swamp C cycle in the region under a changing climate.

## 1 Introduction

15

20

Temperate swamps are known to contribute substantially to the peatland C cycle even though the coverage of this ecosystem is largely underestimated and understudied (Davidson et al., 2022; Kendall et al., 2020). A recent modelling study indicated that many aspects of a swamp's thermal, hydrological and biogeochemical conditions could be adequately modelled, gaining insight into the ecosystem's response to disturbance (Afolabi et al., 2025); however, parameter estimation remained difficult given the scarcity of previous studies in swamps. Process-based models have been widely applied to diverse ecosystems because of their ability to simulate important interactions and feedbacks between biophysical processes and biogeochemical cycles (He et al., 2016; Wang et al., 2022). This model class heavily relies on forcing variables and exact boundary conditions



60



to simulate important processes in forested ecosystems that may be difficult to delineate because of measurement limitations (Munro et al., 2000; Svensson et al., 2008; Yuan et al., 2023). Process-based models also require well-defined parameter values (Silva et al., 2024) but the course of assigning parameter values to important processes in data sparse ecosystems such as temperate swamps can be challenging, thus creating parameter uncertainty when simulating temperate swamp C fluxes and its controlling conditions. Uncertainty in swamp C flux modelling is also introduced from field observations that are used for calibration and validation processes. Large spatial variability across temperate swamps, scaling of instantaneous measurements to daily resolution, varying measurement techniques for different study periods, and overall scarcity of measurements (Davidson et al., 2019; Kendall et al., 2020) influence C flux modelling. Furthermore, observation sparsity and limited modelling studies on swamps to date may also create uncertainties when selecting the appropriate model structure for simulating swamp C balance. Consequently, these uncertainties that are linked to parameterization, field measurement error and model structure all affect the C modelling process of this ecosystem.

Modelling studies have shown that there are interrelationships between biogeochemical and biophysical processes in peatlands. Metzger et al. (2016b, 2016a) reported that simulated C flux variables (e.g., ecosystem respiration and gross primary productivity) are linked to diverse ecohydrological processes (e.g., soil moisture content, soil heat flow, and phenological changes). These interconnections and feedbacks were reflected in the sensitivities of simulated water, energy and C fluxes to diverse process categories such as plant growth and development, soil hydrology, organic matter decomposition, and soil thermal processes. In a similar manner, Yuan et al. (2023) also noted in their modelling study on tropical swamps that plantrelated parameters significantly influenced the energy and C fluxes of their studied area. Understanding the interrelationships and feedbacks that exist within and between biophysical and biogeochemical processes and their parameters through sensitivity analysis is important for model calibration (especially parameter specification) (Muleta & Nicklow, 2005). However, these interactions are not well studied in temperate swamp peatlands with unique hydroperiods, vegetation cover and other biophysical conditions (Davidson et al., 2022; Kendall et al., 2020). Instead, existing modelling studies (e.g., He et al., 2021; Metzger et al., 2015 & 2016a) focused on the interactions in other peatland categories (e.g., bogs and fens) and climatic regions. The modelling study of Afolabi et al. (2025) attempted to fill some of these knowledge gaps by highlighting the relationships between soil respiration and biophysical controls over four decades in a temperate swamp. However, their study did not quantify the uncertainties associated with the measurements used as driving variables and for defining boundary conditions. For instance, they relied on proxy gauging station data to quantify the lateral water influx of a nearby dam and creeks into the studied swamp. This data source may have introduced uncertainties in the swamp's boundary conditions. In addition, because their study relied on local sensitivity analysis (one-at-a-time) approach, some of the non-linear and multi-process interactions may not have been captured. These interactions are important in swamps where a single parameter can influence multiple processes (Yuan et al., 2023). To improve on the limitations of local sensitivity analysis, the global sensitivity analysis (GSA) approach has been adopted by many modelling studies (KC et al., 2021; Wu et al., 2019). Instead of varying just an input or parameter and holding others constant, GSA simultaneously varies all the selected parameters and inputs of a model to help study all plausible interactions between parameters and processes (Hamby, 1994). This procedure assists in identifying



65

80

85

90

95



sensitive and important parameters that are required for calibration and also the assignment of uncertainty level to individual model inputs and parameters, as uncertainty analysis is an essential aspect of any modelling process.

Uncertainty analysis accounts for all the sources of uncertainty and their influence on modelling outcomes that consequently determine the usefulness of model predictions (Muleta & Nicklow, 2005). This analysis may also assist with ranking important processes for field measurement campaigns (Metzger et al., 2016a; Wu et al., 2019) and the parameterization of swamp category in large scale models (e.g., CLASSIC and CAMP) (Bona et al., 2020; Melton et al., 2020). However, no uncertainty analysis has been completed for temperate swamp modelling studies. Therefore, this study undertook an uncertainty analysis of simulated swamp C flux and controls by CoupModel using the Generalized Likelihood Uncertainty Estimation (GLUE) approach to improve our understanding of the dynamic interactions that occur in temperate swamp C cycle. The GLUE method is a systematic approach that captures all sources of uncertainties (Yang et al., 2018) and it is based on the principles of equifinality that finds the plausible combinations of models, parameters and variables that are acceptable for reproducing C flux processes and controlling conditions (Beven, 2006; Beven & Freer, 2001). Consequently, the objectives of this study were to: i) complete a global sensitivity analysis and model calibration with multiple variables (e.g., soil respiration, water table level and leaf area index, ii) present acceptable model structure and parameter distribution for simulating temperate swamp C, which would be an important foundation for predicting future climate change impacts on this ecosystem, iii) identify parameter equifinality and the influence of these parameters on simulated variables, iv) evaluate GLUE performance for simulated variables and suggest measurement variables that will improve our understanding of the soil respiration process in temperate swamps, and v) analyze the sensitivity of swamp C fluxes to changes in lateral water inputs.

Based on literature, we hypothesize that the application of GLUE methodology will improve the initial simulations of Afolabi et al. (2025). We expect that the parameters related to soil organic C decomposition, soil thermal conditions, hydrology, and plant processes will significantly affect soil respiration simulations as suggested by existing studies (e.g., Metzger et al., 2016) that are focused on similar ecosystems (e.g., bogs and fens). We also hypothesize that the swamp's C flux will be responsive to variation in lateral water fluxes.

## 2 Materials and methods

# 2.1 Brief description of study location

Beverly Swamp is a minerotrophic forested wetland situated in Southwest Ontario, Canada (43.366N, 80.12W) with an elevation range of 265 to 270 m. The 2000 ha swamp is a product of an underlying impermeable marl layer that is situated in a double dolomite bedrock depression (Woo, 1987). This unique formation supports a perched water table and the accumulation of ~85 cm peat layer as vegetative productivity exceeded the rate of decomposition (Munro, 1979; Woo & Valverde, 1981). Beverly Swamp is located within the humid continental climate zone with an annual average temperature of 7.6 °C and precipitation of 973 mm (*Canadian Climate Normals 1980-2010*, 2024), Millgrove station). The swamp has a heterogenous canopy cover of both deciduous (e.g., red maple and birch) and coniferous vegetation (e.g., white cedar), and it is mainly



105



drained by two streams, namely Spencer and Fletcher located in the northwest and northeast portions of the swamp, respectively (Woo & Valverde, 1981; Woo, 1987). Detailed description of the site can be found in Appendix A (Table A.1); (Afolabi et al., 2025); (Woo & Valverde, 1981) and other publications cited therein.

## 2.2 Field measurements used for study

## 2.2.1 Forcing variables and initializing measurements

Forty years of daily meteorological measurements (Jan 1983 - May 2023), including, precipitation, air temperature, wind speed, relative humidity, and global radiation were collected from weather stations located within 25 km radius of the swamp (e.g. Valens, Christie Conservation, Hamilton RBG CS and Hamilton A) (see Table 1). Additional observation data sourced from (Munro, 1987, 1989; Munro et al., 2000) were also employed for gap-filling during 1983 - 1986. Other suitable meteorological products such as Ontario in-filled climate data (1983 - 2005) (Ontario Government, 2019), NASA Power Project (1986-2023) (Sparks, 2018) and CWEEDS (1986-2023) solar radiation product of Environment Canada were used to support precipitation and global radiation datasets, respectively as shown in Table 1.

Table 1 Forcing and initialization variables for CoupModel

Variable	Period	Temporal	Data source	Remarks
		resolution		
Air	Jan 1983-May	Daily	Weather station	Details of collection method are
temperature	2023		Munro 1987, 1989	available on Environment Canada's
			and Munro et al.,	website
			2000	< https://climate.weather.gc.ca/histor
				ical_data/search_historic_data_e.ht
				ml>. Additional collection approach
				for support data are described in
				Munro 1987, 1989 & Munro et al.,
				2000





Precipitation	Jan 1983-May	Daily	Weather station	
	2023		Munro 1987, 1989	As described above
			and Munro et al.,	
			2000	
Wind speed	Jan 1983-May	Daily	Weather station	
	2023		Munro 1987, 1989	As described above
			and Munro et al.,	
			2000	
Relative	Jan 1983-May	Daily	Weather station	
humidity	2023		Munro 1987, 1989	As described above
			and Munro et al.,	
			2000	
Global	Jan 1983-May	Daily	NASA Power &	Approach adopted by NASA Power
radiation	2023		CWEEDS	(Sparks, 2018) and Environment
			Environment	Canada
			Canada product	(https://climate.weather.gc.ca/prods
			Munro 1987, 1989	servs/engineering e.html).
			and Munro et al.,	Addition data collection approach is
			2000	described in Munro 1987, 1989 and
				Munro et al., 2000





Volumetric	Jan 1983-May	Daily	Westover gaug	ing Details of collection method are
discharge	2023		station	available on Water Survey Canada
(flow)				<
				>
C content per	1998-2000	One time	McCarter et	al., Analysed with loss on ignition
soil layer			2024	approach
				https://wateroffice.ec.gc.ca/mainm
				enu/historical_data_index_e.html

The climatic variables described were used as dynamic driving variables for CoupModel, while a streamflow dataset from Westover gauging station at the exit of swamp was used as proxy for lateral flow input into the swamp because of the unavailability of this information. To quantify the inconsistencies associated with the lateral flow proxy data assumption, an uncertainty analysis was undertaken for this input variable, which was introduced into the model as average flow input defined by the parameter of *Gwsourceflow*,  $q_{sof}$  (see section 2.4.2 for details). For the initialization process, soil organic carbon (SOC) measurements of depths 0–150 cm that were analysed with loss on ignition approach (McCarter et al., 2024) was used in the model. Details of other site characteristics used for the initialization process are included in Appendix A (Table A.1) and supplementary material (S2).

#### 2.2.2 Measurements used for calibration and validation process

Hourly soil temperature measurements obtained by thermocouples (Type E) at depths (0 – 40 cm); groundwater table level data (barometrically corrected) collected by pressure transducer (Solinst levelogger); and volumetric moisture contents (0-30 cm) of the soil measured by installed Campbell Scientific (CS616) probes across the swamp were used as calibration and validation datasets. Details of compiled calibration and validation datasets are presented in Table 2

## Table 2 Observational datasets for calibration (cal) and validation (val)

Variable	Period	Time scale	Mean ±Std	Data source	Remarks on approach
Soil	1983-1987 (cal);	Daily	Cal: 5.9±6 °C	Field	Obtained with thermocouple
temperature	2022 - 2023 (val)		Val (5cm):	measurement	installation. See Munro
			9.0±7.6 °C		1987, Munro 1989; Munro





Water Table   1983–1987 (cal);   Daily   Cal:-2±19cm   Field   Dotained with pressure   transducer (water level loggers). See Munro 1987,   Munro 1989; Munro et al., 2000; Afolabi et al. (2025) for details				Val (30cm):		et al., 2000; Afolabi et al.
Water Table   1983–1987 (cal);   Daily   Val: 22±21cm   measurement   transducer (water level loggers). See Munro 1989; Munro et al., 2000; Afolabi et al. (2025) for details				l ` ´		· · ·
Level   2022 - 2023 (cal)   Val: 22±21cm   measurement   transducer (water level loggers). See Munro 1987, Munro 1989; Munro et al., 2000; Afolabi et al. (2025) for details						(= = = )
Level   2022 - 2023 (cal)   Val: 22±21cm   measurement   transducer (water level loggers). See Munro 1987, Munro 1989; Munro et al., 2000; Afolabi et al. (2025) for details						
Volumetric   2022-2023 (cal)   Daily   VMC5:69±9.5%   Field   Obtained with corrected time-domain measurement method. See Afolabi et al. (2025) for details	Water Table	1983-1987 (cal);	Daily	Cal:-2±19cm	Field	Obtained with pressure
Volumetric   Moisture   Content   Daily   VMC 30:78±15%   Field   Moisture	Level	2022 - 2023 (cal)		Val: 22±21cm	measurement	transducer (water level
Volumetric   2022-2023 (cal)   Daily   VMC5:69±9.5%   Field   Obtained with corrected   time-domain measurement   method. See Afolabi et al. (2025) for details						loggers). See Munro 1987,
Volumetric Moisture         2022-2023 (cal)         Daily Pointer Designation         VMC 30:78±15% Pield VMC 30:78±15%         Field Time-domain measurement method. See Afolabi et al. (2025) for details           Soil         1998-2000 (cal); Pointer Prespiration         Bi-weekly Pointer Prespiration Prespiration         Cal:10.3±7.6 (Davidson et al., 2019; Pointer Prespiration Pre						Munro 1989; Munro et al.,
Volumetric Moisture         2022-2023 (cal)         Daily         VMC5:69±9.5% (vMC 30:78±15%)         Field time-domain measurement method. See Afolabi et al. Afolabi et al. (2025) for details           Soil         1998-2000 (cal); Pespiration         Bi-weekly 2022-2023 (val) val;4.4±5.4         Cal:10.3±7.6 gC m² d¹ al., 2019; val:4.4±5.4         Obtained with closed opaque chamber method. Spatial variability of same day measurements are ±3.7 gC m² d¹ for val period           Net radiation         1983-1987 (cal)         Daily         7.7±5.7 Mumro 1987, Mumro 1989, and Mumro et al., 2000         Obtained with Bowen ratio approach approach approach approach and Mumro et al., 2000           Latent Heat         1983-1987 (cal)         Daily         4.7±4 Mumro 1987, Mumro 1989, and Mumro et al., 2000         Obtained with Bowen ratio approach approach approach approach approach approach and Mumro et al., 2000         Obtained with Bowen ratio approach approach approach approach approach approach approach and Mumro et al., 2000           Sensible         1983-1987 (cal)         Daily         2.5±1.6 Mumro 1987, Mumro 1989 and Mumro et al., 2000         Obtained with Bowen ratio approach approach approach approach approach approach approach approach approach and Mumro et al., 2000						2000; Afolabi et al. (2025)
Moisture Content         Image: Content Content Content Content         VMC 30:78±15% VMC 30:78±16%						for details
Content         Latent Heat         1983−1987(cal)         Daily         4.7 ± 4         Munro 1987, MJ m²² d¹¹         Obtained with Bowen ratio and Munro et al., 2000           Sensible         1983−1987(cal)         Daily         4.7 ± 4         Munro 1987, MJ m²² d¹¹         Obtained with Bowen ratio approach and Munro et al., 2000           Munro 1987, MJ m²² d¹¹         Munro 1988, and Munro et al., 2000         Obtained with Bowen ratio approach and Munro et al., 2000           Munro 1988, and Munro et al., 2000         Munro 1988, and Munro et al., 2000         Obtained with Bowen ratio approach and Munro et al., 2000           Munro 1989, and Munro et al., 2000         Munro 1988, and Munro et al., 2000         Obtained with Bowen ratio approach and Munro et al., 2000           Munro 1989, and Munro et al., 2000          Munro 1989, and Munro et al., 2000         Munro 1989, and Munro et al., 2000	Volumetric	2022-2023 (cal)	Daily	VMC5:69±9.5%	Field	Obtained with corrected
Net radiation   1983–1987(cal)   Daily   4.7 ± 4   Munro   1987   Afolabi et al. (2025) for details	Moisture			VMC 30:78±15%	measurement	time-domain measurement
Soil         1998-2000 (cal);         Bi-weekly         Cal:10.3±7.6         (Davidson et opaque chamber method. with closed opaque chamber method. Spatial variability of same day measurements are ±3.7 gC m² d¹¹           Respiration         1983-1987 (cal)         Daily         7.7 ± 5.7 Munro 1989 and Munro et al., 2000         Munro 1989 and Munro et al., 2000         Obtained with Bowen ratio approach and Munro et al., 2000           Latent Heat         1983-1987 (cal)         Daily         4.7 ± 4 Munro 1989 and Munro et al., 2000         Munro 1989 approach and Munro et al., 2000         Obtained with Bowen ratio approach and Munro et al., 2000           Sensible         1983-1987 (cal)         Daily         2.5 ± 1.6 Munro 1989 and Munro et al., 2000         Obtained with Bowen ratio approach and Munro et al., 2000           Munro 1989 and Munro et al., 2000         Munro 1989 and Munro et al., 2000         Munro 1989 approach approach and Munro et al., 2000	Content					method. See Afolabi et al.
Soil         1998-2000 (cal); respiration         Bi-weekly 2022-2023 (val)         Cal:10.3±7.6 gC m <sup>-2</sup> d <sup>-1</sup> al., 2019; val:4.4±5.4 gC m <sup>-2</sup> d <sup>-1</sup> (Davidson et al., 2019; val:4.4±5.4 schmidt & spatial variability of same day measurements are ±3.7 gC m <sup>-2</sup> d <sup>-1</sup> for cal and ±1.8 gC m <sup>-2</sup> d <sup>-1</sup> for val period           Net radiation         1983–1987 (cal)         Daily         7.7±5.7 MJ m <sup>-2</sup> d <sup>-1</sup> Munro 1987, and Munro et al., 2000         Obtained with Bowen ratio approach and Munro et al., 2000           Latent Heat         1983–1987 (cal)         Daily         4.7±4 Munro 1989, and Munro et al., 2000         Obtained with Bowen ratio approach and Munro et al., 2000           Sensible         1983–1987 (cal)         Daily         2.5±1.6 Munro 1989, and Munro 1989, and Munro 1989, and Munro et al., 2000         Obtained with Bowen ratio approach approach approach approach and Munro et al., 2000						Afolabi et al. (2025) for
Respiration   2022-2023 (val)   gC m <sup>-2</sup> d <sup>-1</sup>   al., 2019; Schmidt & Spatial variability of same day measurements are ±3.7 gC m <sup>-2</sup> d <sup>-1</sup> for cal and ±1.8 gC m <sup>-2</sup> d <sup>-1</sup> for val period   Munro 1987, MJ m <sup>-2</sup> d <sup>-1</sup>   Munro 1987, Obtained with Bowen ratio approach and Munro et al., 2000   Munro 1989 approach   Munro 1989 approach   Munro 1989 and Munro et al., 2000   Munro 1989 approach   Munro 1989 and Munro et al., 2000   Munro 1989 approach   Munro 1989 ap						details
Net radiation       1983–1987 (cal)       Daily       7.7 ± 5.7 MJ m²² d¹¹       Munro 1987, and Munro et al., 2000       Obtained with Bowen ratio approach         Latent Heat       1983–1987 (cal)       Daily       4.7 ± 4 MJ m²² d¹¹       Munro 1987, MJ m²² d¹¹       Obtained with Bowen ratio approach         Sensible       1983–1987 (cal)       Daily       2.5 ± 1.6 MJ m²² d¹¹       Munro 1987, Munro 1987, and Munro et al., 2000       Obtained with Bowen ratio approach         Munro 1987, and Munro et al., 2000       Munro 1989, approach       Approach         Munro 1987, and Munro et al., 2000       Munro 1987, and Munro et al., 2000       Obtained with Bowen ratio approach         Munro 1989, and Munro et al., 2000       Munro 1989, approach       Audition of the second of the secon	Soil	1998-2000 (cal);	Bi-weekly	Cal:10.3±7.6	(Davidson et	Obtained with closed
Strack, 2026    Strack, 2026    day measurements are ±3.7   gC m <sup>-2</sup> d <sup>-1</sup> for cal and ±1.8   gC m <sup>-2</sup> d <sup>-1</sup> for val period	respiration	2022-2023 (val)		gC m <sup>-2</sup> d <sup>-1</sup>	al., 2019;	opaque chamber method.
Net radiation   1983 – 1987 (cal)   Daily   7.7 ± 5.7   Munro   1987   Obtained with Bowen ratio   MJ m <sup>-2</sup> d <sup>-1</sup>   Munro   1989   approach   and Munro   et   al., 2000				val:4.4±5.4	Schmidt &	Spatial variability of same
Net radiation         1983−1987 (cal)         Daily         7.7 ± 5.7 Munro         Munro         1987, approach         Obtained with Bowen ratio approach           Latent Heat         1983−1987 (cal)         Daily         4.7 ± 4 Munro         Munro         1987, Obtained with Bowen ratio approach           MJ m⁻² d⁻¹         Munro         1989 approach           and Munro         1989 approach           and Munro         1989 approach           Sensible         1983−1987 (cal)         Daily         2.5 ± 1.6 Munro         Munro         1987, Obtained with Bowen ratio           Heat         MJ m⁻² d⁻¹         Munro         1987, Obtained with Bowen ratio           and Munro         1989 approach           and Munro         1989 approach				gC m <sup>-2</sup> d <sup>-1</sup>	Strack, 2026)	day measurements are ±3.7
Net radiation         1983−1987 (cal)         Daily         7.7 ± 5.7 Munro         Munro         1987, and Munro et al., 2000         Obtained with Bowen ratio approach           Latent Heat         1983−1987 (cal)         Daily         4.7 ± 4 Munro         1987, Munro et al., 2000         Obtained with Bowen ratio approach           Sensible         1983−1987 (cal)         Daily         2.5 ± 1.6 Munro et al., 2000         Munro et al., 2000         Obtained with Bowen ratio approach           Heat         MJ m⁻² d⁻¹         Munro et and						gC m <sup>-2</sup> d <sup>-1</sup> for cal and $\pm 1.8$
MJ m <sup>-2</sup> d <sup>-1</sup>   Munro 1989   approach						gC m <sup>-2</sup> d <sup>-1</sup> for val period
Latent Heat   1983–1987(cal)   Daily   4.7 ± 4   Munro   1987,   Obtained with Bowen ratio   MJ m <sup>-2</sup> d <sup>-1</sup>   Munro   1989   approach   and Munro   et   al., 2000	Net radiation	1983-1987 (cal)	Daily	$7.7 \pm 5.7$	Munro 1987,	Obtained with Bowen ratio
Latent Heat $1983-1987$ (cal)       Daily $4.7 \pm 4$ Munro $1987$ , Munro $1989$ approach and Munro et al., $2000$ Munro $1989$ approach and Munro et al., $2000$ Sensible Heat $1983-1987$ (cal)       Daily $2.5 \pm 1.6$ Munro $1987$ , Munro $1987$ , Obtained with Bowen ratio approach and Munro et and Munro et approach				MJ m <sup>-2</sup> d <sup>-1</sup>	Munro 1989	approach
Latent Heat         1983-1987 (cal)         Daily         4.7 ± 4         Munro 1987, Munro 1989 approach         Obtained with Bowen ratio approach           Sensible         1983-1987 (cal)         Daily         2.5 ± 1.6 Munro 1987, Munro 1987, Munro 1989 approach         Obtained with Bowen ratio approach           Heat         MJ m <sup>-2</sup> d <sup>-1</sup> Munro 1989 approach         Approach					and Munro et	
$\begin{array}{c ccccccccccccccccccccccccccccccccccc$					al., 2000	
$ \begin{array}{c ccccccccccccccccccccccccccccccccccc$	Latent Heat	1983-1987 (cal)	Daily	$4.7 \pm 4$	Munro 1987,	Obtained with Bowen ratio
Sensible   1983 – 1987 (cal)   Daily   2.5 ± 1.6   Munro   1987,   Obtained with Bowen ratio   Munro   1989   approach   and Munro   et				MJ m <sup>-2</sup> d <sup>-1</sup>	Munro 1989	approach
Sensible 1983–1987 (cal) Daily 2.5 ± 1.6 Munro 1987, Obtained with Bowen ratio  Heat MJ m <sup>-2</sup> d <sup>-1</sup> Munro 1989 approach  and Munro et					and Munro et	
Heat MJ m <sup>-2</sup> d <sup>-1</sup> Munro 1989 approach and Munro et					al., 2000	
and Munro et	Sensible	1983-1987 (cal)	Daily	$2.5 \pm 1.6$	Munro 1987,	Obtained with Bowen ratio
	Heat			MJ m <sup>-2</sup> d <sup>-1</sup>	Munro 1989	approach
al., 2000					and Munro et	
					al., 2000	





LAI	1998 (cal)	seasonally	3.9±1.9	Thambipillai	Obtained with ground-based
				1998	measurements and
					hemispherical photography
Snow Depth	1983 – 1987 (cal)	seasonally	24±16 cm	Munro 1987,	Obtained during snow
				Munro 1989	survey
				and Munro et	
				al., 2000	

Additional datasets were sourced from existing studies as compiled in Table 2. Bi-weekly soil CO<sub>2</sub> flux measurements were obtained by closed opaque chamber method and analyzed with gas chromatograph (1998-2000) or measured directly (2022-2023) with LI-COR portable greenhouse gas analyzer (LI-7810) (Davidson et al., 2019; Schmidt & Strack, 2026). Historic hourly measurements of net radiation, ground heat, sensible heat, latent heat fluxes derived by Bowen ratio surface energy and additional measurements of water table level, soil temperature (0–5 cm) and snow depth were sourced from (Munro, 1987, 1989; Munro et al., 2000). Compilation of measured Leaf Area Index (1998) by direct measurement and hemispherical photography were sourced from Thambipillai (1998). Detailed measurement methodologies are published in the papers compiled in Table 2.

## 135 **2.3 Modelling approach**

130

140

145

150

## 2.3.1 CoupModel description

CoupModel (coupled model), a one-dimensional coupled heat and mass transfer model that simulates thermal and hydrological conditions of ecosystems and the adjoining biological processes that mediates C exchange between the atmosphere, vegetation and soil environment (Jansson & Moon, 2001; Jansson & Karlberg, 2004), was adopted for this study. In particular, the CoupModel version 6 (CoupModel v6) (He et al., 2021) which is an upgrade of the previous versions used for existing studies such as Metzger et al. (2016a) was adopted for this research. The estimation of heat and water flow processes in CoupModel are based on the laws of conservation of energy and mass and flows of thermal energy (Fourier's law) and water (Richard's equation) created by gradient differences in temperature and water potential. C balance simulations and plant development in the model are products of the interactions between plants and forcing hydroclimatic variables (Svensson et al., 2008). CoupModel consists of many biotic and abiotic sub-modules for radiation and precipitation interception, evaporation and transpiration, snow and surface water pools, soil temperature and heat fluxes, plant growth and maintenance, soil hydraulics, and soil organic C decomposition (Jansson & Moon, 2001; Jansson & Karlberg, 2004; Metzger et al., 2016b, 2016a; Jansson, 2012) (see eqs. A1- A52 of Supplementary Materials (S1 & S3) for details of functions used to simulate the processes). Detailed description of the model can be accessed in (Jansson & Karlberg, 2004; Jansson, 2012) and other publications referenced therein.



155

160

165

180



# 2.3.2 Model design and setup for Beverly Swamp

The model set-up and parameterization for this study is based on the previous use of CoupModel at Beverly Swamp as described in Afolabi et al. (2025). Parameter assignment was informed by field measurements, lab experiments, literature values, experience from single runs and default model values (See Table 4 and S2). In particular, Simulations were started five years (1978–1982) prior to study period (1983) with repeated forcing variables of first 5 years (1983–1987) to allow the system adapt to site conditions and make it less dependent on initial values as adopted by Metzger et al. (2016a, 2016b). The soil profile for Beverly Swamp was divided into thirteen layers varying in thickness between 5 cm (0-30 cm depth), 10 cm (30-50 cm), 15 cm (50-80 cm), 20 cm (80-120cm) and 30 cm (120 -150cm) intervals. We simulated ~1 m peat depth because the topmost layer of the swamp has an average peat layer of 85 cm (50-100 cm thick) that is underlined by an almost impermeable marl layer (Munro et al., 2000). Sub-modules of global radiation and precipitation interception, surface pool formulation and snowmelt were used to define the swamp's soil surface boundary conditions (Jansson & Karlberg, 2004; Metzger et al., 2016a). Energy fluxes (net radiation, sensible and latent) of the swamp were simulated by an iterative solution of the energy balance that captures the feedback between moisture availability and temperature (eqs. A1-A4 in S1). However, for soil surface temperature, convection was switched off because previous research (Smith & Woo, 1986) has shown that vertical conduction is the dominant heat flow mechanism in Beverly Swamp. Annual average air temperature and amplitude of 7.64 °C and 12 °C, respectively were adopted for estimating the bottom boundary conditions for heat conduction in Beverly Swamp (eqs. A9-A11 in S1). This heat conduction, energy flux and air temperature also interacted with other simulated processes (e.g., snow pack). Details of the specific equations and parameters used can be found in supplementary material (S1 & S3).

## 2.3.2.1 Soil hydraulic and lateral water flow at Beverly swamp

The van Genutchen Model (vGM) soil water retention curve (van Genuchten, 1980) (eq. A14 in S1) was used to represent the soil water potential and soil moisture content relationships of the swamp's 13 soil layers, while the Mualemequation (Mualem, 1976) (eq. A15 in S1) defined the unsaturated hydraulic conductivity of the swamp's soil (eqs. A12-A22 in S1). These two functions were used to simulate vertical water movement through the swamp's soil matrix as it conforms with Darcy's law (Richards, 1931). Values of van Genutchen's empirical parameters used for the simulation were estimated with pedotransfer functions (Letts et al., 2000; Liu & Lennartz, 2019) using dry bulk density measurements (Czerneda, 1985; Munro, 1982). Residual water content and wilting point parameters were estimated from literature (Dimitrov et al., 2010; Letts et al., 2000; Menberu et al., 2021).

The perched nature of the swamp supports water accumulation, and the point of soil saturation (water table level, WTL) as it rises above the drainage datum is marked by continuous saturation from the WTL to the marl layer which signifies the bottom of the soil profile. Hydraulic conductivity at the marl layer is as low as 0.86 mm/day (McCarter et al., 2024; Warren et al., 2001) with no significant interaction with regional groundwater flow (Macrae et al., 2011; Valverde, 1978). As the simulated WTL rises over the marked drainage datum (e.g., WL in draining Fletcher and Spencer streams), water efflux of the saturated



185

190

195

200

205

210

215



peat layers above the marked level was linearly simulated (eq. A22 in S1) (Metzger et al., 2016a). The addition and loss of water from adjacent soil layer was used to maintain saturation level in simulation similar to ground water field measurements (Metzger, 2015). The swamp's runoff was driven by the generated water pool at soil surface that accumulates when water in the surface layer of the soil is transmitted upwards during completely saturated condition and when throughfall exceeds the rate of infiltration. Ultimately, runoff was a function of the water produced in the surface pool and the estimation of the swamp's soil moisture depended on water storage and temperature (Metzger et al., 2015, 2016a; Wu et al., 2011). In addition to the simulations above, a two-domain approach (not ordinary Darcy's flow) that takes into consideration a bypass of the micropore soil matrix flow system (Jansson et al., 2005) was also tested for the flow process at Beverly swamp (eqs. A19 – A21 in S1).

## 2.3.2.2 Vegetation and soil organic carbon of the swamp

In CoupModel, vegetation was represented by an "explicitly bigleaf' model (5-10 m height) with a single representative canopy layer characterized by the closed canopy structure (LAI of  $\sim$ 5-6) in the swamp with a root depth of  $\sim$ 30 cm (Table A1). No understory vegetation was simulated since cover was low and thus insignificant for the simulated C and hydrology fluxes. The plants represented in the model are divided into different parts of leaf, stem, root, grain and mobile pools but for this simulation, grain allocation was excluded because of its insignificant contribution in non-agricultural settings (Metzger et al., 2016b). The initial vegetation conditions used for the simulation were based on the field measurements computed in Table A1. The lightuse efficiency sub-model, which considers the proportionality between plant growth and global radiation and the limitations imposed by moisture availability, temperature and nitrogen supply was used to simulate the swamp's photosynthetic rate and C assimilation of the swamp's vegetation (eqs. A23 – A26 & A39 – A43 in S1) (Jansson & Karlberg, 2004; Wu et al., 2011). A fixed N approach was used, which means that the nutrient limitation for the plant growth was implicitly included in the specified light use efficiency parameter. The model simulated leaf area index, surface albedo, root depth and other plant characteristics dynamically (eq 41). These properties feedbacks to micrometeorological conditions that consequently alter local climate and hydrology. Plant respiration simulation for the swamp is assumed to be a function of both maintenance and growth and was estimated from the functional trait coefficients (Amthor, 1984; Amthor & Baldocchi, 2001; Cannell & Thornley, 2000; Jansson & Karlberg, 2004) of the swamp species and was further regulated by air temperature. See eq. A23-A24 in S1 & S3 for model equations and parameters that are related to plant processes.

The SOC initialization process for Beverly Swamp was based on methods adopted by several previous studies that define conditions in the soil layer (Dangal et al., 2022; He et al., 2023; Metzger et al., 2015, 2016a) and not the common "spin-up" approach. Spin-ups will not produce realistic results for this simulation because "equilibrium" may not be achieved in disturbed (i.e., known peat extraction, road and transmission line construction) peat soils like Beverly swamp where the humified pool will take multiple decades to restabilize (Byun et al., 2018; Woo, 1979; Woo, 1987), thus affecting SOC pool and fluxes (Nemo et al., 2017). To account for this in CoupModel, the swamp's SOC was partitioned into 13 layers (see S2). The initial C and nitrogen content per layer were assigned by measurements and partitioned into two SOC pools (litter and slow turn over /



220

225

230



recalcitrant) for each of the layers based on their C:N ration and extent of decomposition (DeSimone, 2009; Schmidt & Strack, 2026; Wang et al., 2015; Webster et al., 2014). This was to ensure that the specified initial conditions fulfilled the measured total C per layer. Beverly Swamp's measured total C storage of ~98 kg/m<sup>2</sup> (McCarter et al., 2024) were separated by reported soil C:N values into active and passive pools to represent the fast and slow turnover rates, respectively. Consequently, high or low C:N for a given soil layer means more fast or slow cycling SOC pool will be initialized, respectively. The swamp's SOC at different depths were partitioned into the two major pools in a manner that is almost at equilibrium for defined parameters coalescence, which eventually generates a realistic fit to soil respiration (Dangal et al., 2022; He, et al., 2023; Metzger et al., 2015, 2016a). For the simulation, decomposition of fast and slow turnover pools were estimated by first-order rate process that is limited by substrate quality, moisture availability and temperature (Jansson et al., 2008; Metzger et al., 2015; Wu et al., 2011) (See eqs. A44 – A52). Temperature sensitivity of microbial decomposition was described by the Q<sub>10</sub> response function given in eq. A46, while that of moisture was controlled by different moisture limits that constraints microbial decomposition when soil is either too dry or wet (eq. A47 in S1) (Metzger et al., 2016b). Therefore, as the swamp litter decomposes, CO<sub>2</sub> is emitted, and soil organic matter is formed. Further decomposition of humus under oxic and more favorable condition (e.g. increased WTD) produces only CO<sub>2</sub>. Also at deeper soil layers, moisture saturated conditions, lower soil temperature and less labile organic matter lower the decomposition rate. Because a static displacement of organic matter between layers was used for this study, there was no downward displacement of C at deeper layers. This means the model structure did not account for vertical peat C movement (He et al., 2023; Jansson & Karlberg, 2004). See eqs. A44 -A52 in S1 and S3 for sub-model functions and parameter values used in SOC simulation.

## 2.4 Sensitivity analysis and calibration process using the GLUE Approach

Field measurements of 1983–1986 and 1998–2000 were used for parameter sensitivity analysis and calibration, while those of 235 2022-2023 were adopted for validation. The single run of the initialized model for the swamp (Afolabi et al., 2025) provided the foundation for this study. To select the parameters for the multiple run analysis, an initial screening (sensitivity analysis) of 90 identified parameters (see S4) representing diverse processes related to plant growth and development, water, energy and C flux processes was completed with the one-factor-at-a-time (OAT) approach described by (Lenhart et al., 2002) (See 240 also figure 1). The process thereafter reduced the final number of selected parameters for calibration to 38 based on their importance and sensitivity to C flux processes, while the remaining ones were held static for the runs (see Table 3 for details). The prior range of parameters presented for GLUE analysis were defined in such a manner to cover anticipated posterior value (Svensson et al., 2008). Thereafter, a total of 35,000 Monte Carlo simulations of random uniform sampling were implemented for the study to generate both prior and posterior distributions covering a broad range of C balance conditions in the swamp. 245 The process assisted in locating possible sets of models, parameters and variables that generate ensemble simulations that match observations (Wu et al., 2013). The ensembles were split into behavioural and non-behavioural simulations (Metzger et al., 2016a) based on their consistent performance as acceptable solutions that fit well with the multiple observed variables described in section 2.2. Consequently, those that fall below set threshold (see section 2.4.1 below) were discarded while the



260

265



ones above were accepted as behavioural simulations. Posterior parameter intervals of between 5<sup>th</sup> to 95<sup>th</sup> percentile of the distribution of parameter values of accepted runs were considered for the study. These posterior distributions generated after applying the acceptance thresholds were compared to the prior distribution to identify sensitive parameters.

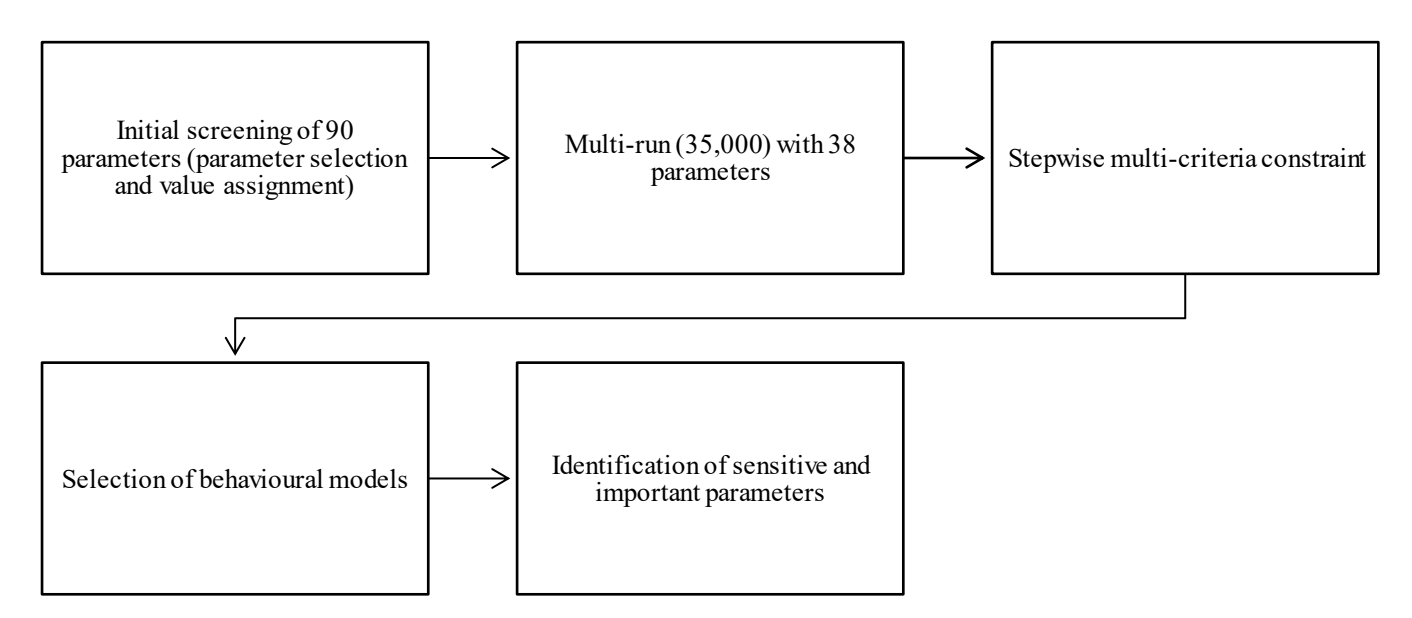


Figure 1. Schematic diagram of the GLUE (GSA and calibration) processes for the study

# 2.4.1 Performance indices, set thresholds and interrelationships

Simulations produced above were constrained to field measurements through the setting of multiple acceptance criteria in the form of performance indices, namely, coefficient of determination (R²) and Mean Error (ME). These two indices have been shown by previous uncertainty studies with the GLUE approach in CoupModel (Metzger et al., 2016a; Wang et al., 2022; Wu et al., 2019) to be effective in capturing all the seasonality and interannual variabilities embedded in simulated and observed datasets with strong influence on the overall process of sensitivity analysis and calibration. R² describes the strength of the relationship that exists between simulated and field measurements by estimating the extent that the variability in simulated data explains that of observations using a regression line (Kalantari et al., 2012). R² is particularly independent of the data scale being considered and the value produced by this statistical index falls with the range of 0 and 1. ME, which tests the bias of the simulation, is the average of all errors generated from the difference between simulated and observed variables as it represents the magnitude of the difference.

For the selection of behavioral models and for the calibration process, measured soil temperature, hydrological measurements (water table level and volumetric moisture content), C fluxes (soil respiration), energy fluxes (net radiation, latent heat and sensible heat), plant properties (LAI), and snow depth were used to constrain the simulations. The setting of the constraining thresholds was inspired by the uncertainty estimated from field measurements (see Table 2) and previous single run experience



290

295



- described in Afolabi et al. (2025). In particular, thresholds of R²>0.80 for soil temperature, R²>0.7 for LAI, R²>0.5 for net radiation flux, R²>0.4 for VMC and soil respiration, R²>0.3 water table level and latent heat flux, R²>0.1 for sensible heat flux, snow depth and surface pool were set as criteria to constrain the selection of acceptable runs. In addition, estimated uncertainty measurement of soil respiration was considered in assigning ME constraint for the simulation. Where ME of ± 0.5 and ±3 g C/m²/d were used to constrain the model for both the validation and calibration periods, respectively. Additional ME
  constraint was only applied to soil respiration because it is the only C flux that was validated for the study and the main C flux variable in the study with much interest for improvement. Furthermore, the simultaneous R² and ME constraints on all the variables led to the rejection of the 35,000 runs.
  - The constraining process was achieved in multiple steps. The above described  $R^2$  and ME thresholds were applied to soil respiration and each of the variables (controls) in a stepwise manner to test the level of constraint each of the variables has on behavioural model selection and soil respiration in particular. Thereafter, all the multiple constraints of the measurement were simultaneously applied. In addition, equifinality (Eq.k. equation 1) between the calibrated parameters of diverse process categories was determined by summing their covariance ( $R^2$ ) as presented in equation 1a (Metzger et al., 2016a; Wu et al., 2019). Only cases where correlation  $\geq 0.4$  were considered for the analysis.

$$Eq_{jk} = \sum 2 \times \frac{2^{10 \times R_{jk}^2 j \neq k}}{10}$$
 Equation 1

- Where  $Eq_{jk}$ , is the equifinality index,  $R_{jk}$  is the correlation between the parameters j and k that are estimated from acceptable models
  - For initial identification of sensitive parameters, Wilcoxon signed rank and Kolmogorov-Smirnov tests were applied to detect the difference between prior and posterior parameters distribution and to also identify the posterior parameters that have been transformed from uniform distribution. In addition, a range ratio index of posterior to prior distribution was also computed after calibration (Wu et al., 2019). After the identification of sensitive parameters, the contribution (importance) of sensitive parameters to the performance of selected simulated variables outputs was quantified using the Lindeman, Merenda and Gold (LMG) approach (Johnson, 2000; Lindeman et al., 1980; Wu et al., 2019). LMG method is an averaging over ordering method that quantifies the proportion of total variance (R<sup>2</sup>) explained by each dependent variable (i.e., model parameters in this case). In this study, the relative weight of the sensitive parameters in the form of proportion of averaged R<sup>2</sup> across the orderings are predictors of studied variables (Equation 2).

$$LMG(x_k) = \frac{1}{p} \sum_{j=0}^{p-1} \left( \sum_{S \subseteq \{x_1, \dots, x_p\} \setminus \{x_k\}} \frac{seqR^2(\{x_k\} \mid S)}{\binom{p-1}{i}} \right)$$
 Equation 2

Where  $seqR^2$  ( $\{Xk\}|S$ ) represents  $R^2$  summation when regressor  $\{Xk\}$  is being added to regression model with the set of regressors S. The implementation of the LMG approach was done with the R package "relaimpo" (Groemping, 2006). Consequently, the completion of the process helped identify and rank sensitive parameters.





# 300 2.4.2 Lateral input variation

To quantify the uncertainty associated with lateral water flow, which is largely influenced by Valens dam and the two creeks draining Beverly swamp, measurements from Westover gauging station were used to specify the prior parameter range representing this variable in CoupModel. This parameter (Gwsourceflow,  $q_{sof}$ ) was calibrated as part of the GLUE process and further varied at different sensitivities ( $\pm 10\%$ ,  $\pm 25\%$ ,  $\pm 50\%$ ) as a separate experiment in the study to test the response of C flux variables to these changes. Selection of sensitivity range for testing was informed by existing hydrological studies in the swamp area (McCarter et al., 2024; Sultana & Coulibaly, 2011).

# 2.4.3 Comparison of Beverly swamp modelling set-up and the previous studies

Even though similar biophysical conditions and biogeochemical cycles of diverse ecosystems were simulated by prior studies using the CoupModel (see Table 3 for comparison), the modelling set-up described above is unique to the Beverly Swamp (temperate swamp peatland ecosystem) in Southern Ontario, and it is one of the first attempt to evaluate the performance of CoupModel in a temperate peatland where the hydroperiods, vegetation cover and other biophysical conditions are distinct. Our experience from Afolabi et al (2025) informed the selection and evaluation of important hydrological components (e.g. surface pool and lateral flow) for the swamp set-up in CoupModel that were not the focus of previous experiments (see Table 3). Initial single model run of the swamp suggested that the surface pool generated when the infiltration capacity of the swamp's top peat layer is exceeded, affected the water table level and partitioning of energy fluxes. These hydrological processes are critical to simulating the swamp ecosystem's water balance, and not those of previous studies because of the difference in their ecosystem (e.g. bogs and fens).

Table 3 Comparison of prior CoupModel set-up

CoupModel version	Ecosystem/ location	Study period	Calibration/evaluation variable	Calibration/ uncertainty method	Evaluation metrics	Reproducibility
CoupModel first generation (Svensson et al 2008)	Spruce forest, Sweden	2001-2004	SH, LH, NR, ST, LAI, NEP, Biomass and Litter	Bayesian- Markov Chain Monte Carlo (10 <sup>4</sup> - 10 <sup>5</sup> runs)	ME	See Svensson et al 2008
CoupModel 4.0 (Metzger et al., 2015)	Treeless peatlands (Finland, UK, Netherlands, Germany	2006-2010	NEE, GPP, Reco, ST, SD, LAI, Biomass	Monte-Carlo (10 <sup>5</sup> runs)	R <sup>2</sup> , ME	See Metzger et al., 2015
CoupModel 5.0 (Metzger et al., 2016)	Oligotrophic, minerogenic mire, Sweden	1991-2013	WTL, LAI, NEE, SH, LH, NR, ST, SD	Monte-Carlo (10 <sup>4</sup> runs)	R <sup>2</sup> , RMSE	See Metzger et al., 2016





CoupModel (Coup-CNP) (I al, 2021)	He et.	Upland forest, Sweden	1961-2081	C: N, N:P, C:P, biomass, DOC	Monte-Carlo (10³ runs for 2 regions)	R <sup>2</sup> , ME	See He et. al, 2021
CoupModel (Svensson et al		Agricultural site, Sweden	1984-2019	Water drainage, soil nitrate, SON	Monte-Carlo (10 <sup>4</sup> runs)	R <sup>2</sup> , ME, RMSE	See Svensson et al 2025
CoupModel 6.0 study)	) (This	Swamp, Canada	1983-2023	ST, WTL (saturation level and surface pool), VMC, Rs, NR, LH, SH, LAI, SD	Monte-Carlo (GLUE Approach, 10 <sup>4</sup> runs)	R <sup>2</sup> , RMSE	See details in Data availability section

Note that SH, LH, NR, ST, LAI, NEP, NEE, GPP, Reco, Rs, SD, LAI, WTL, C:N, N:P, C:P, DOC and SON are acronyms for sensible heat flux, latent heat flux, net radiation flux, soil temperature, leaf area index, net ecosystem production, gross primary production, ecosystem respiration, soil respiration, snow depth, leaf area index, water table level, carbon to nitrogen, ni trogen to phosphorus ratio, carbon to phosphorus, dissolved organic carbon and soil organic nitrogen respectively.

#### **325 3 Results**

330

335

340

## 3.1 Calibrated parameters and sensitivities

The GLUE Calibration process transformed most of the uniform parameter distribution of the prior to other distributions (e.g. normal and log normal) in the posterior. Out of the 38 parameters selected for calibration, 17 showed a very significant difference (p < 0.05) between prior uniform distribution and posterior distribution before multicriteria constraint. However, this number increased to 24 after selection of behavioural models as shown in Table 4. The sensitive parameters resulting from the calibration procedure were linked to diverse biotic and abiotic categories controlling plant properties, soil organic processes, soil thermal dynamics, soil water storage and transport, land surface energy exchanges, and other physical processes. In particular, all the parameters in the soil organic matter category showed significant sensitivity with reduced posterior mean for litter  $(K_1)$  and humus  $(K_h)$  decomposition rates but an increase for surface litter decomposition  $(L_1)$  after calibration. Comparing the ratio of mean posterior distribution to prior (range ratio) in Table 4, RateCoefHumus (K<sub>h</sub>, 0.37, decomposition rate of humus), RateCoefLitter (K<sub>1</sub>, 0.44, decomposition rate of litter), LeafRate1 (1<sub>Lc1</sub>, 0.60, leaf litter fall), MobileAlloCoef (m<sub>retain</sub>, 0.60, mobile allocation of the vegetation) and AlbedoV (a<sub>veg</sub>, 0.69, albedo of the vegetation) showed the largest changes. This result is not unprecedented because K1 and Kh parameters are important to the decomposition of labile C and the recalcitrant humus layer of peat soil, respectively, thus influencing soil C efflux. Conversely, a decrease was observed in the posterior distribution value of  $l_{Lc1}$  parameter after calibration.  $l_{Lc1}$  constrains the leaf litter fall process during non-autumnal period with strong influence on litter abundance and the rate at which it disappears or is transferred to humus. Posterior distribution value of m<sub>retain</sub> parameter increased after calibration with more allocation to mobile C pool. m<sub>retain</sub> influences the storage of non-structural carbohydrates and its allocation during the non-growing season or under extreme conditions (Jansson





& Karlberg, 2004). This parameter therefore has a strong relationship with forest gross primary productivity. The calibration process produced a lower posterior mean value for a<sub>veg</sub> parameter, which affects the amount of shortwave radiation that is reflected from the heterogenous canopy structure of Beverly Swamp. a<sub>veg</sub> is a major driver of energy flux partitioning of land-surface energy exchange, which eventually affects thermal conditions and evapotranspiration mechanisms in forested ecosystems. Overall, the presented results of the global sensitivity analysis (GSA) and calibration process assisted in identifying sensitive parameters and the parameter distribution for modelling water, energy and C fluxes in temperate swamp ecosystems. It is noteworthy that the adoption of the Global Sensitivity Analysis (GSA) approach for this study assisted in mapping sensitive and important parameters for simulating the swamp's C fluxes and controlling conditions, identifying essential parameter interactions and their equifinality. These unique findings were not identified by previous studies (e.g. Afolabi et al., 2025) because they utilized the typical local / OAT analysis which inherently focuses on linear interactions.





Table 4: Prior and posterior parameter distribution after calibration (See SMPs 1 & 2 for detailed parameter definitions)

Parameter function	Parameter definition	Prior range	ange	Prior	Post	Range
ૹ				mean	mean	$ratio^1$
Symbol		Min	Max			
Plant Processes						
MCoefCoarseRoot	Maintenance resniration coefficient for coarse root					
(Kmrespcoarseroot)	Mannenance respination coefficient for coalse 1000	0.0001	0.02	0.01	0.004	0.93
RadEfficiency (e <sub>L</sub> )	Radiation use efficiency; rate of photosynthesis	2.8	4	3.40	3.33	96.0
Leafc1 (lc1)	Fraction of new assimilates which is allocated to the leaves	0.1	0.4	0.25	0.24	0.77
	Rate coefficient for the leaf litter fall before the first threshold					
LeafRate1 (l <sub>Lc1</sub> )	temperature sum tL1 is reached	0.00001	0.01	0.01	0.001	9.0
I anf Pote 7 (1. a)	Rate coefficient for the leaf litter fall after the second threshold					
Lamaica (1Lc2)	temperature sum tL2 is reached	0.01	0.1	90.0	90.0	0.97
GrowthCoef(kgrep)	Growth respiration coefficient	0.1	0.3	0.20	0.19	0.93
LAI enh Coef	Scaling factor for enhanced leaf litter fall rates when higher					
$(LAI_{enhCoef})$	LAI values are reached	0	1	0.50	0.65	0.85
Mobile Allo Coef (mretain)	Mobile allocation of the vegetation	0.3	0.95	0.63	0.85	9.0
Rootlowestdepth (pzroot)	Lowest depth of root	-0.5	-0.2	-0.35	-0.34	0.94
SpecificLeafArea	Factor for calculating LAI from leaf biomass, which is the					
$(p_{l,sp})$	inverse of specific leaf area	50	120	85	06	0.95
AlbedoV (a <sub>veg</sub> )	Albedo of vegetation	10	20	15	14	69.0
Soil Organic Processes	Sess					

<sup>1</sup> Range ratio is the posterior parameter distribution relative to the prior





RateCoefHumus	Decomposition rate of humus coefficient					
$(k_h)$		0.000001	0.0001	5E-05	0.004	0.37
RateCoefLitter1	Decomposition rate of litter coefficient					
$(k_1)$		0.0001	0.01	0.005	0.01	0.44
RateCoefSurfL1	Decomposition rate of surface litter coefficient					
(III)		0.5		0.75	06.0	0.91
Land surface exchange processes	inge processes					
Albedo Wet (awet)	Albedo of wet soil	10	20	15	14	6.0
Conduct VPD	Vapour pressure deficit that corresponds to 50% reduction of					
$(g_{\mathrm{vpd}})$	stomata conductance	10	200	105	115	0.81
Conduct Max	Maximum stomatal conductance					
(gmax)		0.009	0.05	0.03	0.03	96.0
Conduct Ris (gris)	Stomatal conductance per leaf area	3E+06	7E+06	5E+06	5E+06	0.74
KBMinusOne (kB-	Canopy turbulence coefficient					
1)		1.5	3	2.25	2.29	0.81
Maximal Cover	Maximal canopy cover					
(c <sub>max</sub> )		0.75	1	0.88	0.87	0.95
Surface and Soil Water Processes	ater Processes					
PrecA0Corr (crain)	Wind correction of rain precipitation	1	1.15	1.08	1.06	0.78
TempCoefA (twA)	Temperature coefficient in the temperature response function.	0.1	3	1.55	1.57	0.87
Airmincontent	Minimum amount of air required to prevent any reduced					
(q <sub>Amin</sub> )	uptake of water from the soil	0	S	2.5	1.73	0.7
SPMaxCover	Maximum surface pool cover					
(p <sub>maxt</sub> )		0.5	1	0.75	08.0	0.88
SurfPoolMax	Water on the soil surface that corresponds to complete cover					
(Wpmax)	of the whole soil.	50	200	125	91	68.0
			٠	•	•	





GWSourceLayer	Layer for the ground water source flow					
$(q_{sol})$		1	4	2.5	2.72	0.95
Total conductivity	Total conductivity at top layer					
$(1)$ $(k_{satl})$		50	2100	1075	1090	0.92
Total conductivity	Total conductivity at middle layer					
(6) (k <sub>sat6</sub> )		9	30	18	20	0.95
GWSourceFlow	Constant rate of ground water source					
$(q_{sof})$		0	1.6	8.0	0.36	0.71
DrainSpacing (dp)	Distance between drainage system	50	2500	1275	1107	6.0
Soil Thermal & Otl	Soil Thermal & Other Abiotic Processes					
ThScaleLog(1)	Scaling coefficient for thermal conductivity					
Xhf		-0.5	0.5	0	-0.06	66.0
MeltCoefAirTemp	Temperature coefficient in the empirical snow melt function					
(m <sub>T</sub> )		1	3	2	2.32	0.87
ThetaPowerCoef	Power coefficient in the response function of microbial					
$(p_{\theta})$	activity in dependency of soil moisture	0.2	2	1.1	0.99	0.95
Saturation activity	Saturation activity in soil moisture response function.					
$(p_{qSatact})$		0.05	0.5	0.28	0.35	0.89
Thetaupperange	Water content interval in the soil moisture response function					
$(b_{\rm qUpp})$	for microbial activity	3	20	12	13	0.82
Theta Lower	Water content interval in the soil moisture response function					
Range (pqLow)	for microbial activity, mineralisation – immobilisation, nitrification and denitrification.	3	20	12	12	0.83
TemQ10Bas	Temperature response function for plant respiration					
$(t_{ m pQ10bas})$		20	35	28	27	6.0
TemQ10 (tQ10)	Respiration response function of temperature	1.5	3	2.3	2.2	0.97



370



## 3.1.1 Equifinality of parameters

Parameter equifinality is at the core of the GLUE approach in identifying parameter sets and interactions that reasonably describe important processes in the modelled system. Summation of R<sup>2</sup> generated from the correlation matrix of calibrated parameters (see S4 for matrix) described in section 2.4 was used to compute the equifinality of this modelling experiment. The overall equifinality of the parameters was categorized into five process groups namely, plant properties, soil organic matter processes, energy balance drivers, soil water processes and soil thermal and other abiotic processes as presented in Figure 2.

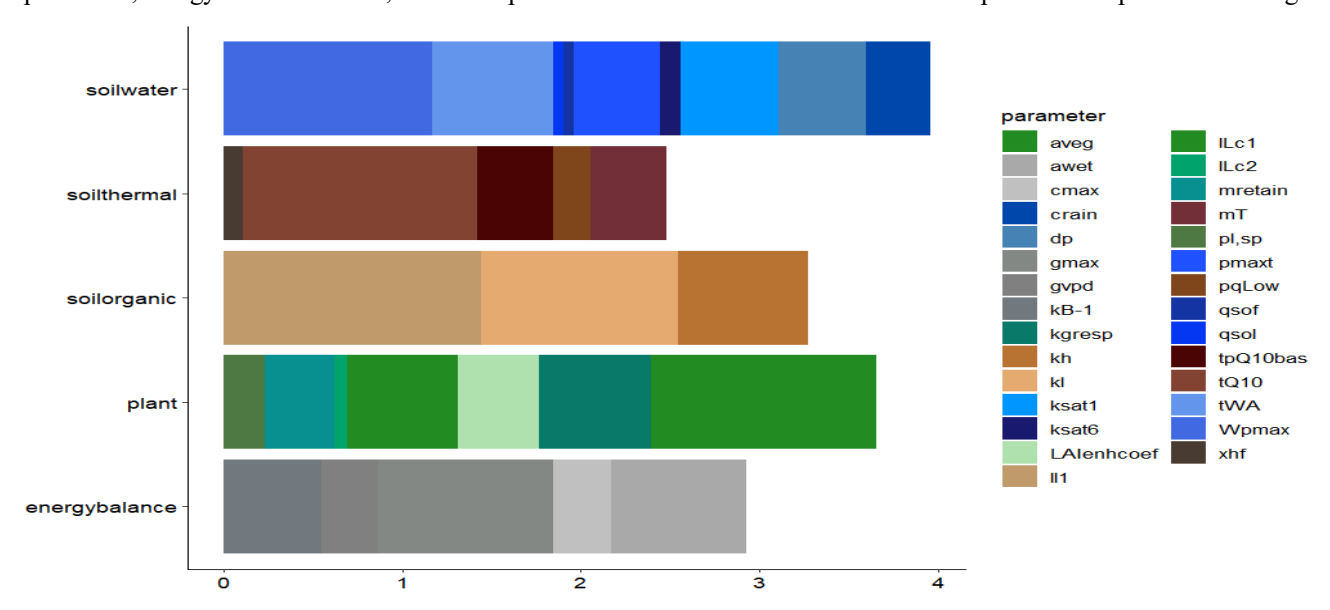


Figure 2. Mean equifinality of calibrated parameter-process categories. Note that chart does not have unit

Considering the average of each category highlighted above, parameters related to soil water processes ranked highest with average equifinality value of 3.96. Within this category, SurfacPoolMax ( $W_{pmax}10.5$ ) accounted for the most equifinality. The category linked to plant processes ranked the next with had mean equifinality value of 3.7, and  $a_{veg}$  (8.9) had the highest equifinality in this group. Parameters in the soil organic matter class were estimated to have an average equifinality of 3.3 with the combination of  $k_1(4.33)$  and  $l_{11}$  (3.3) accounting for almost 80 percent of the total equifinality in the group. Energy balance category (2.9) and soil thermal and other abiotic group (2.5) had the lowest mean equifinality for the computed correlation matrix. Generally, more equifinality was observed between parameters of the same process category than those of other categories.

## 375 3.1.2 Parameter influence on variable simulation

In determining the influence of sensitive parameters on simulated variables, the normalized relative weight ( $R^2$  average) of the parameters derived from the LMG method (described in section 2.4) and their contribution to model performance are presented in Figure 3.



390

395



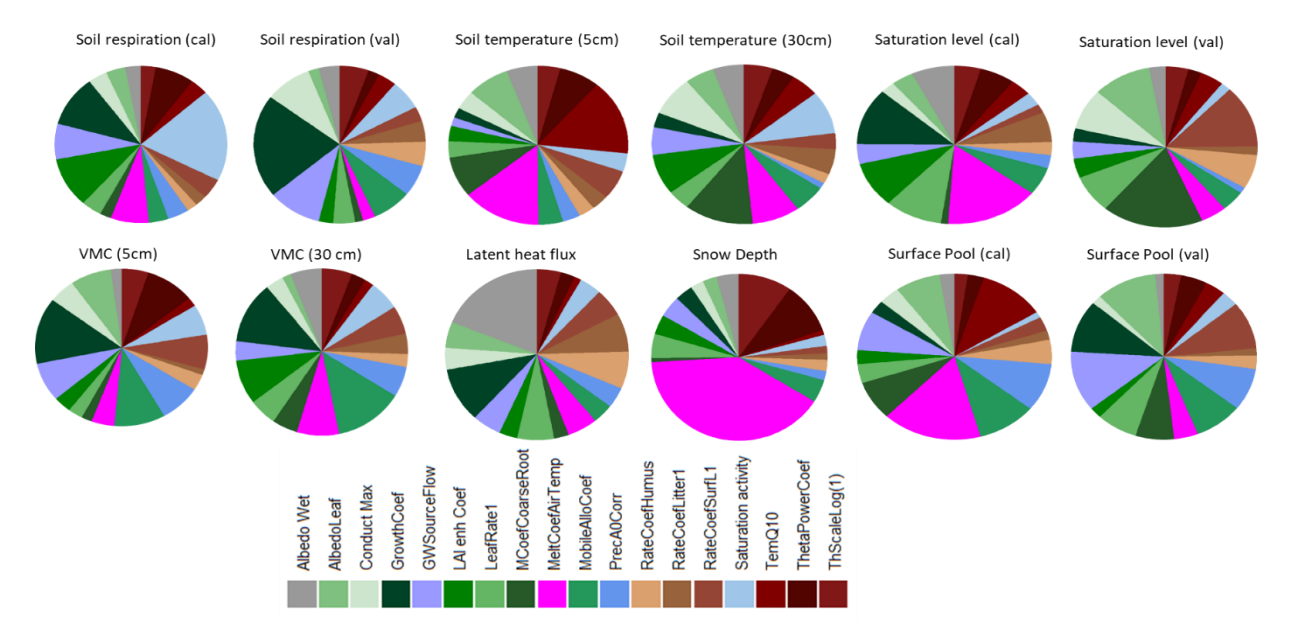
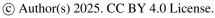


Figure 3. Parameter contribution to variable performance (R<sup>2</sup>), where cal & val represents calibration and validation periods, respectively. See also S5 for details and also the definition of parameters

The simulated variables showed sensitivities to parameters of different categories but the parameters representing plant growth (Growthcoef, kgresp), soil water drainage/input (GWSourceFlow, qsof) processes and snow melt (MeltCoefAirTemp, mT) exerted the strongest influence on all the simulated variables. Soil respiration simulations were most sensitive to plant growth (kgresp), soil moisture response function (saturation activity, pqSatact) and soil water drainage (qsof) parameters but with some variations between the calibration (1998-2000) and validation (2022-2023) period. The calibration period showed high sensitivity to both p<sub>qSatact</sub> and k<sub>gresp</sub> parameters, while q<sub>sof</sub> and k<sub>gresp</sub> parameters were the highest for the validation period. For the simulation of hydrological variables (saturation level, volumetric moisture content and surface pool), plant related coefficients (McoefCoarseRoot, kmrespcoarseroot; kgresp; MobileAlloCoef, mretain), snow melt (mT) and soil water drainage (qsof) parameters contributed the most to explaining the variability in these simulated variables. However, the parameter sensitivity differed for both the calibration and validation periods for both the saturation level and surface pool simulations. The variability in net radiation, latent heat and sensible heat flux simulations were most explained by parameters representing radiation properties (albedo wet,  $a_{wet}$ ) and soil moisture response ( $p_{qSatact}$ , thetapowercoef,  $p_{\theta p}$ ). Respiration response function of temperature ( $t_{Q10}$ ), respiration parameter of coarse root (kmrspcoarseroot) and snowmelt related coefficient (m<sub>T</sub>) parameters ranked top in explaining the variabilities in soil temperature and snow depth simulations, while plant related parameters (LAI enhcoef and kmrespooarseroot) ranked the most in explaining the variability in LAI. Overall, parameters of diverse process categories exerted influence on C, water and energy flux modelling performance at Beverly Swamp. This influence was more prominent in situations where parameters and variables shared the same process category.





# 3.2. Evaluation of model performance following the GLUE approach to parameter estimation

The systematic GLUE approach assisted in identifying the ensemble sets of parameters with the highest likelihood to match 400 measurement data in section 2.2. Out of the 35,000 prior simulations that were completed, only 30 ensembles were accepted as behavioural simulations for the posterior distribution after applying all the stringent multicriteria thresholds adopted for the experiment. The ensemble mean of the posterior models performed better than that of the simulations generated by the prior distribution as represented by Table 5.

# Table 5 Performance (R2) of prior and posterior models

Variable	N	Distribut =35000	ion prior	selection	Distribu	ıtion post se	election =30
		Mean	CV	Range	Mean	CV	Range
Soil temperature (5cm) cal	707	0.86	0.20	0.93	0.89	0.01	0.05
Soil temperature (5cm) val	343	0.92	0.20	0.97	0.93	0.02	0.07
Soil temperature (30cm) val	344	0.88	0.20	0.94	0.90	0.02	0.07
Saturation level (cal)	1066	0.48	0.37	0.73	0.55	0.25	0.53
Saturation level (val)	348	0.35	0.74	0.78	0.65	0.04	0.15
VMC (5cm)	346	0.45	0.59	0.94	0.78	0.09	0.27
VMC (30cm)	346	0.16	1.28	0.74	0.52	0.12	0.27
Soil respiration (cal)	88	0.25	0.41	0.63	0.30	0.16	0.32
Soil respiration (val)	10	0.43	0.49	0.98	0.72	0.18	0.45
Net radiation	840	0.70	0.20	0.76	0.73	0.01	0.05
Latent heat flux	840	0.41	0.36	0.71	0.50	0.18	0.45
Sensible heat flux	840	0.20	0.38	0.50	0.24	0.17	0.41
Leaf area index	57	0.50	0.47	0.93	0.74	0.06	0.13
Snow depth	36	0.54	0.23	0.71	0.52	0.13	0.40
Surface pool (cal)	1067	0.09	0.96	0.48	0.24	0.38	0.54
Surface pool (val)	347	0.42	0.34	0.84	0.54	0.27	0.49

<sup>\*</sup>CV represents coefficient of variation while cal and val denote calibration and validation periods



415

420

425



# 3.2.1 Soil respiration

The GLUE approach reduced the uncertainty of posterior soil respiration simulations (Table 5). Soil respiration simulations showed significant improvement as represented by the changes in mean R<sup>2</sup> (0.43 to 0.72) and ME (-2 to 0 gC m<sup>-2</sup> d<sup>-1</sup>) in prior and posterior models, respectively during the validation period. In fact, soil respiration showed the greatest observed improvement after multiple constraints compared to the other studied variables, and when compared to the result of the single run (See Table B1 in Appendix). This is an indicator of higher uncertainties in simulating soil respiration. The accepted models were mostly able to represent the seasonality in soil respiration of both the calibration and validation periods (Figure 4). However, some of the peaks in soil respiration rate in late spring and early summer were not well captured by the posterior model ensemble when compared to field measurement. This mismatch is not unexpected because soil respiration is highly influenced by plant processes, hydrology, and thermal conditions, so the inadequacies from the simulation of these controls will cascade into soil respiration and other C flux simulations.

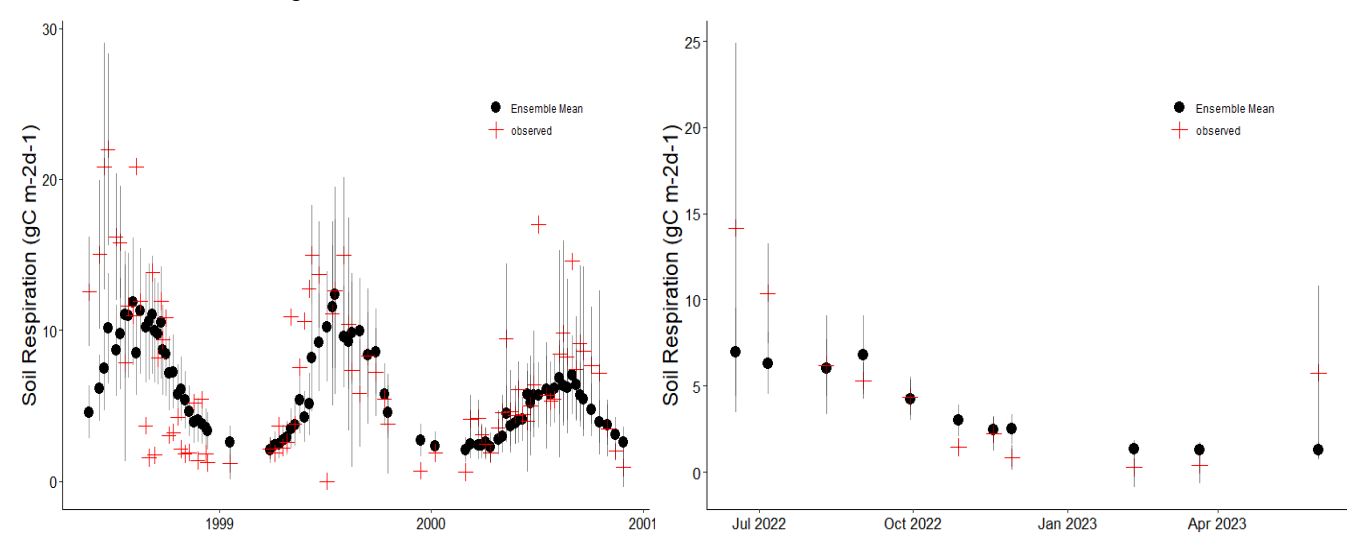


Figure 4. Plot of observation against ensemble mean of simulated soil respiration for calibration (1998 – 2000) and validation (2022 – 2023) periods. Error bars in black reflect the standard deviation of measured soil respiration (black), while those in red represent the standard deviation of the acceptable models

Compared to the calibration period, soil respiration was better simulated in the validation period with less uncertainty than the calibrated period ( $R^2$  of 0.3 and ME: -1.1 gCm<sup>-2</sup>d<sup>-1</sup>). This may be linked to measurement error, difference in collection approach and spatial variability during this period and the uncertainties that also cascaded from controlling variables. The magnitude of uncertainty related to measurements was also reflected by the spatial variability of soil respiration data across the installed soil fluxing sampling locations with standard deviation values of 3.7 gCm<sup>-2</sup>d<sup>-1</sup>for calibration (1998 – 2000) and 1.8 gCm<sup>-2</sup>d<sup>-1</sup> (2022 – 2023) for the validation periods.



435

440

445



## 3.2.2 Hydrological simulations of the swamp

The calibration process significantly improved the simulation performance of the hydrological variables (i.e., water table level and volumetric moisture content) and to a greater extent than soil temperature. This is an indication that the simulation of the hydrological variables is more uncertain than that of soil temperature. In comparison to the prior models, saturation level and surface pool (water table level) simulations showed higher mean R<sup>2</sup> (0.65; 0.54) and reduced ME (0.02m; -5 mm) in the posterior model ensemble, respectively for the validation period as shown in Table 5. However, the partitioning of WTL shows that saturation level was better simulated than surface pool (see Table 4 and Figure 5). For the saturation level and surface pool simulations, the validation period was better simulated than calibration period. Peak drought generated during very dry summer and autumn years (1985 and 2022) were not well captured in the saturation level simulations. These, and other inaccurate representations in the system's behaviour, cumulatively made simulated saturated level slightly lower than that of observation. Similar underestimation was also observed in the surface pool simulation when compared to the observed data. Some of these inadequacies may be linked to that the fact the model was mostly trained with wet years during the calibration period (1983 – 1986), so it was unable to fully capture the extremely dry conditions presented in the validation period (e.g., 2022)

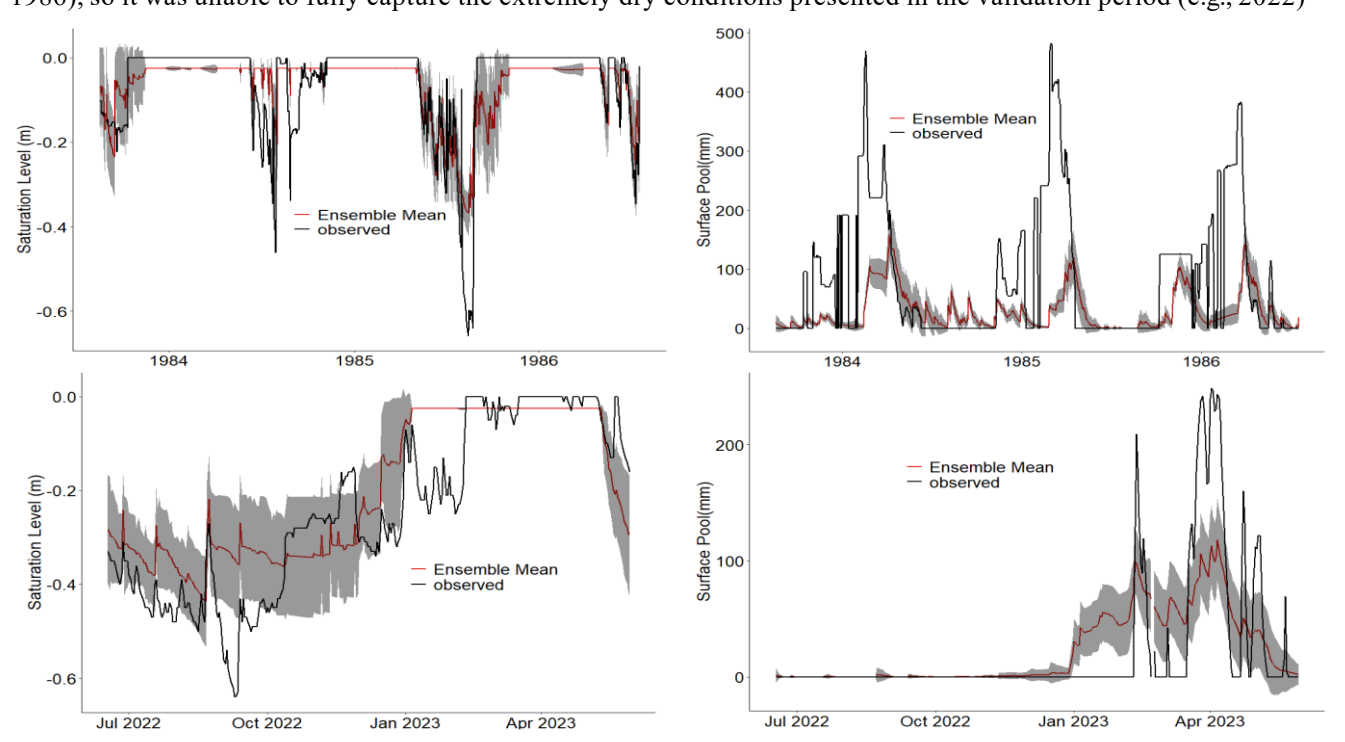


Figure 5. Observation versus ensemble mean of saturation and surface pool simulations for calibration (a) and validation (b) periods

For the posterior model,  $R^2$  value of simulated VMC at 5 cm (0.45 to 0.78) and 30 cm (0.16 to 0.52) increased but ME values also increased. The 5 cm VMC matched better with observation than that of 30 cm with mean  $R^2$  of  $\geq$ .63 and  $\geq$ 0.41, respectively. However, more moisture deficit was simulated for the topsoil than that of middle layer as presented in Figure B1.



450

455

460

465

470



## 3.2.3 Soil temperature and snow simulation

Overall, posterior simulation of soil temperature ranked highest when compared to measured data with 90-93% of the variability in measured soil temperature explained by those of the simulated (see Table 5). This is an improvement from the initial  $R^2$  range of 0.88-0.92 in the prior distribution with middle layer (30 cm) showing more evident improvement than the surface layer (5 cm). For the accepted simulations, soil temperature at the two layers were overestimated during the summer seasons, while the lowest temperatures in winter were not perfectly captured (See Figure B1). The overestimation in summer may be linked to moisture underestimation during this period, which results in more partitioning into sensible heat than latent heat. Also, the pattern of snow disappearance may not be well represented in the model so this may have affected model-observation fit during winter. Unlike soil temperature simulation, the GLUE approach did not result in a significant difference in snow depth simulation. Instead, a slight reduction in fit to measured data ( $R^2$  from 0.54 to 0.52) was observed in the posterior. This reduction may be associated with the overestimation of snow accumulation in the first year of the simulated period and the seasonal mismatch that results from snow accumulation and disappearance during the winter season. Despite the slight reduction in fit to measured data for the GLUE calibrated snow depth simulation, the  $R^2$  (0.54) value was still higher than the result of the single run in Table B1 (Appendix).

## 3.2.4 Energy balance performance

The performance of all the simulated energy flux components, namely net radiation latent heat and sensible heat fluxes improved after calibration as shown by their  $R^2$  values. However, latent heat flux experienced the most improvement from mean  $R^2$  of 0.4 to 0.5 and reduction in mean error from -0.8 MJ m<sup>-2</sup> d<sup>-1</sup> to -0.5 MJ m<sup>-2</sup> d<sup>-1</sup> (see Table 5). Most of the measured seasons were captured well by the posterior model except for the underestimation during the spring season of the calibration period (See Figure B2). This underestimation in spring led to the partitioning of more energy to sensible heat flux. Generally, sensible heat flux simulation did not perform as well as latent heat flux, with overestimation in summer and autumn and underestimation in spring when compared to measured data. This cumulatively contributed to the mismatch between observed and simulated sensible heat flux with mean  $R^2$  and ME values of 0.24 and 0.12MJ m<sup>-2</sup> d<sup>-1</sup>, respectively. Net radiation had the highest mean  $R^2$  (0.73) and ME (1.21 MJ m<sup>-2</sup> d<sup>-1</sup>) among the three simulated energy fluxes. The high  $R^2$  value can be linked to the good fit between simulated and observed data for most of the calibrated period. However, there was some underestimation and overestimation of net radiation during spring and summer seasons, respectively in some of the studied years (e.g., spring 1984). This seasonal mismatch was then also reflected in simulated latent and sensible heat fluxes.

# 3.2.5 Evaluating the results of prior single run and GLUE calibration results

Compared to the single run of Afolabi et al. (2025), the GLUE approach improved some of the simulated variables but did not affect others, and in some cases, the calibration process diminished their performance (see Table B1 and Figure B4). For instance, the R<sup>2</sup> (0.72) and ME (-0.02 gC m<sup>-2</sup> d<sup>-1</sup>) of GLUE simulated (mean of behavioural models) soil respiration improved



485

495



from the initial single run values of 0.58 and 0.45 gC m<sup>-2</sup> d<sup>-1</sup> respectively (see Figure B4). This confirmed that the stringent performance constraint of the GLUE set-up on this variable reduced the mean error by over 100%. Also, the R<sup>2</sup> (0.65) and ME (1.7 cm) of GLUE simulated saturation level improved from the initial single run values of 0.58 (R<sup>2</sup>) and 21cm (ME) respectively. However, the R<sup>2</sup> (0.35) and ME (2.4 MJ m<sup>-2</sup> d<sup>-1</sup>) of GLUE simulated sensible heat flux diminished from the initial single run values of 0.35 (R<sup>2</sup>) and 2.4 MJ m<sup>-2</sup> d<sup>-1</sup> (ME). The compared results should be interpreted with caution because the performance range of the GLUE calibrated results is dependent on the selection threshold outlined in section 2.4.1. for constraining the simulations. For example, R<sup>2</sup>>0.80 was set as the constraining threshold for soil temperature in the GLUE experiment, which is lower than the R<sup>2</sup> (0.95) value of the single run. Furthermore, ME constraint was only applied to soil respiration and not the other variables, so this may greatly affect the GLUE calibrated results. It is also possible that the stringent multicriteria constraint of the GLUE calibration improved some of the simulated variables at the expense of others. See Table B1 in the Appendix section for the comparison of other variables.

## 3.3 Experiment of constraining variables on soil respiration flux

When the R<sup>2</sup> constraints described in section 2.4 were applied to only soil respiration, ~53% of the prior simulations were rejected (Figure 6). The stepwise addition of soil thermal, hydrological, and plant variable constraints to soil respiration led to model rejection rates of 53% (constrained for soil temperature in addition to soil respiration), 53% (snow depth), 91% (WTL), 92% (VMC) and 85% (LAI). Although VMC showed the strongest individual constraint on acceptance rate, the combination of soil water related variables (WTL and VMC) produced a stronger model rejection value of 96%.

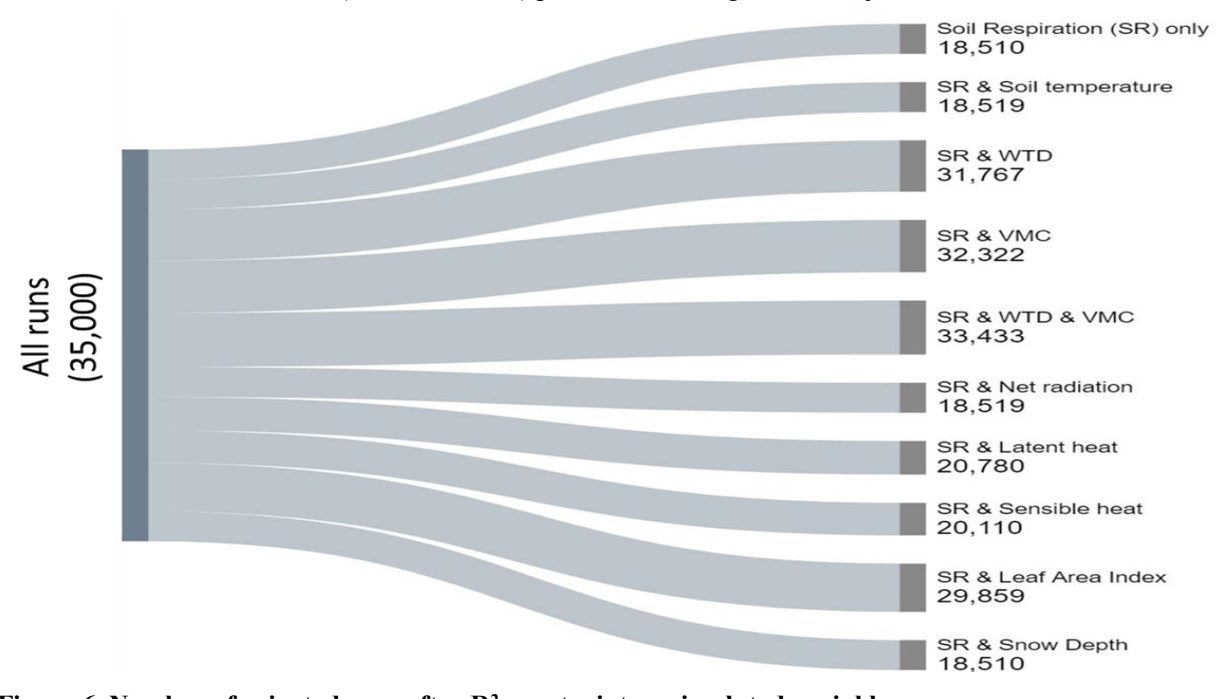


Figure 6. Number of rejected runs after R<sup>2</sup> constraint on simulated variables



505

510

515



For the energy flux variables, combining soil respiration constraints with these variables produced rejection rates of 53% (net radiation), 59% (latent heat) and 57% (sensible heat flux). This shows that latent heat flux produced the strongest constraint on the acceptance rate of the behavioral models for energy fluxes. This may be linked to the uniqueness of latent heat flux in representing the energy flux component of evapotranspiration that couples both energy and water balance. A similar result was observed for all the variables when ME constraint was added to the R<sup>2</sup> constraint of soil respiration as presented in Figure B3. However, LAI ranked higher than VMC or WTL in constraining the prior simulations.

## 3.4 Importance of lateral water flux

Lateral flow is an important variable for defining boundary conditions for modelling energy, water and carbon fluxes in Beverly Swamp. The variation experiment of lateral water input ( $\pm 10\%$ ,  $\pm 25\%$  and  $\pm 50\%$ ) showed that gross primary productivity, ecosystem respiration and net ecosystem exchange simulations were responsive to lateral water flux changes as shown in Figure 7. One-tenth and one-quarter increase in lateral input resulted in  $\leq 1\%$  increase in GPP and Reco and 1% increase in NEE, while one-half increase raised GPP, Reco and NEE values by 2.5%, 2% and 4%, respectively. For the reverse experiment, one-tenth reduction in the lateral input led to less than 1% decline in GPP, Reco and NEE, while one-quarter and one-half reduction in water flux further declined GPP by 2%-5%, Reco by 2%-4% and NEE by 4%-6% respectively. This experiment shows that the swamp's C flux displayed minimal sensitivity to changes in lateral water input.

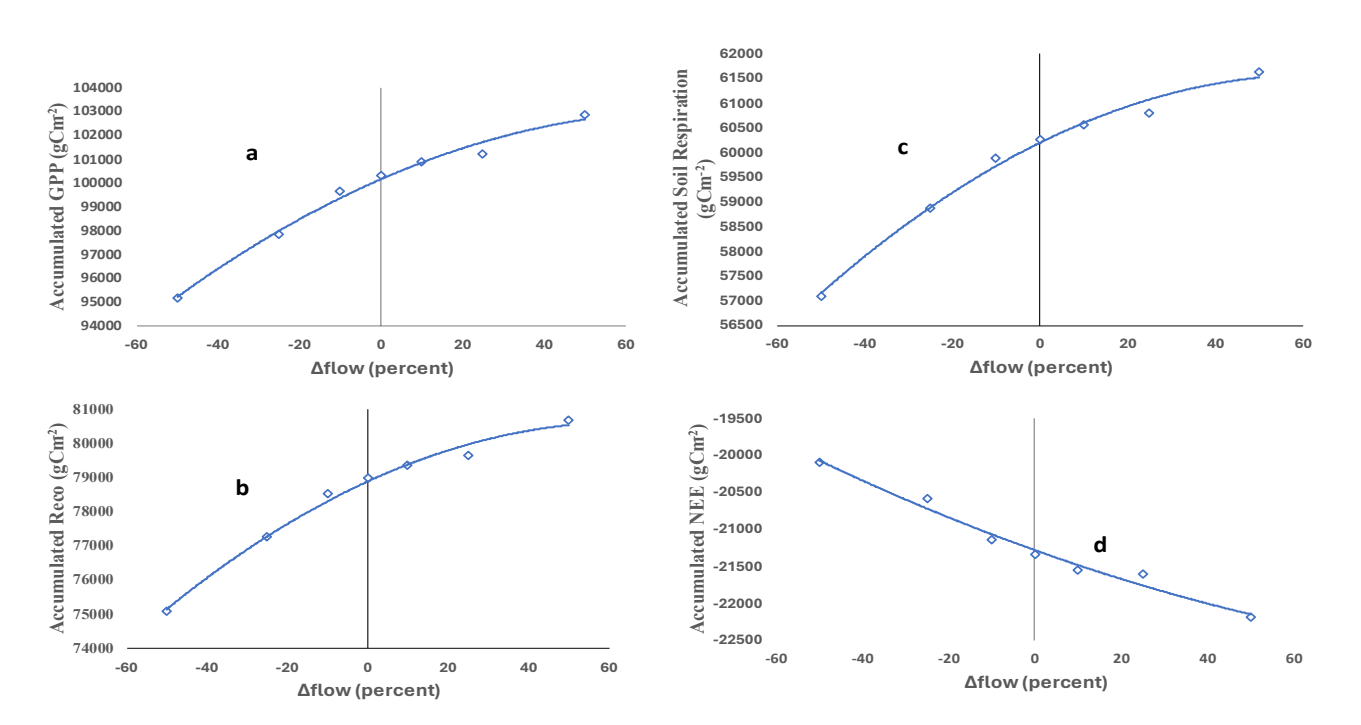


Figure 7. Response of Accumulated GPP (a), ecosystem respiration (b), soil respiration (c) and NEE (d) to lateral water input variation over 40 years (1983 – 2023)





#### 4 Discussion

520

525

530

535

540

545

The adoption of the GLUE approach for this study reduced some of the uncertainties associated with temperate swamp C modelling as highlighted in Section 3.2. This confirms part of the hypothesis presented in the introduction section of this study that GLUE will help achieve this. Global sensitivity analysis and calibration process of GLUE assisted in mapping parameter distribution, constraining boundary conditions and identifying sensitive and important parameters for simulating water, energy and C fluxes in a temperate swamp peatland. The approach reduced the margin of parameter uncertainty in this ecosystem, where parameter values required for modelling C flux and relevant controls are not readily available (Yuan et al., 2023). Critical boundary conditions such as later water flux was better constrained by the process than when parameterization was done one-at-a-time (e.g., Afolabi et al., 2025). In addition to the GLUE results, the sensitivity analysis experiments of constraining variables for soil respiration and C flux response to lateral flow variation (Sections 3.3 and 3.4) also confirmed our other hypotheses on the interconnections that exist between the different ecohydrological processes within this temperate swamp ecosystem. However, the extent of the interactions and the contribution of each process category to C flux and biophysical conditions simulation varied.

#### 4.1 Parameter-process influence on soil respiration simulation

As described in the Results (Section 3.1), soil respiration simulations were mostly sensitive to plant growth respiration (kgresp), soil moisture response function (pqSatact) and soil water drainage (qsof) parameters. kgresp coefficient, which represents the concentration of C efflux per C assimilated as structural dry matter, constraints autotrophic respiration in the model (Jansson & Karlberg, 2004; Lavigne & Ryan, 1997). k<sub>gresp</sub> is dependent on plant functional traits, canopy age and size (Schmiege et al., 2023) and is linked to many critical processes such as plant productivity, tissue nitrogen content, root respiration and rhizosphere (Litton et al., 2007; Ryan, 1990) that control soil respiration processes in swamps. This finding is consistent with other studies that reported the strong influence of this parameter on C flux variables (Hanson et al., 2000; Metzger et al., 2016b). The other two parameters that soil respiration responded to with strong sensitivity were hydrology related. Numerous studies have shown that hydrology is a strong mediator of soil respiration as it exerts control on almost all the processes related to soil respiration in temperate swamps (Davidson et al., 2019; Kendall et al., 2020). In particular, the parameter soil water drainage (q<sub>sof</sub>), which represents later water flow input into the swamp, displayed strong influence on soil respiration. The importance of this parameter corroborates the results of other modelling studies (Ju et al., 2006; Tonkin et al., 2018) and the findings of the lateral flow variation experiment in section 3.4. Lateral water flux is an important part of the soil water balance of Beverly Swamp with water sources from Fletcher and Spencer creeks that drain the swamp, and the influence of regulated flow supplies from Valens dam upstream of the swamp (McCarter et al., 2024; Woo & Valverde, 1981). Flow variation of this water flux showed that soil respiration and other C flux components are sensitive to lateral flow variation even though at a reduced magnitude. Nevertheless, the 3% increase in soil respiration rates when lateral flow was increased from 0 to 50% can be attributed to soil moisture abundance that was initially limiting. Moisture deficit impedes plant productivity, substrate



550

555

560

565

570

575

580



availability, microbial activities and other mechanisms constraining soil respiration process (Blodau, 2002; Limpens et al., 2008). Therefore, future disturbances from dam operations and climate change that alter lateral flow regimes of the swamp is also expected to offset its C dynamics. Furthermore, while the lateral flow experiment presented here represents shifts in plant and microbial activity in response to resulting soil moisture change, persistent shifts to lateral flow regimes could result in succession of the plant community (Tonkin et al., 2018) that would have consequent impacts on swamp C cycling. Even though the simulation performance of soil respiration was influenced by plant and hydrology related parameters, there were variations in the parameter influence for the calibration (1998-2000) and validation (2022-2023) periods. The greater sensitivity of the calibration period to soil moisture response function ( $p_{qSatact}$ ) and plant growth respiration ( $k_{gresp}$ ), and that of validation to soil water drainage (qsof) and plant growth respiration kgresp parameters may be linked to the spatial variability that exist in swamps. The different sections of Beverly Swamp have distinct hydrogeomorphic settings that influence the hydrology and vegetation distribution of the swamp (Davidson et al., 2019; McCarter et al., 2024; Woo & Valverde, 1981). Therefore, the collection of soil respiration measurements at different points in the swamp with distinct local ecohydrological characteristics may have introduced the variability in soil respiration data used for calibration and validation. In addition, interannual variability may also have affected the water availability of the study periods and its effect on soil respiration process. Consequently, this finding possibly explains the origin of the spatial variability in field measurements, which cascaded into the model assessment process.

## 4.2 Parameter equifinality in swamp C flux model

In addition to parameters' influence on model performance, the result of parameter equifinality described in section 3.1.1 was also used to understand the interactions between plant processes, soil organic matter cycling, hydrological processes, energy flux drivers, soil thermal conditions, and other abiotic processes in Bevely Swamp. Substantial parameter equifinality was observed in the modelling of the swamp's water fluxes, energy balance and C flux components. Some of the parameters showed single interconnection, while others showed high equifinality. Parameters related to soil water (SPMaxCover, pmax; SurfPoolMax, W<sub>pmax</sub>) and plant (LeafRate 1, 1<sub>Lc1</sub>) process categories ranked highest in equifinality. This result is in line with the findings of Yuan et al. (2023) where they observed that swamp C flux variables were sensitive to plant (phenology) parameters. Also, the posterior distribution of some calibrated parameters of this study (e.g.,RateCoefLitter1) are similar to those presented by other studies (Metzger et al., 2016), even though the experiments were undertaken in other peatlands (e.g., fens). Despite the similarities, the equifinality analysis confirms that the interactions between sets of parameters take priority over individual parameters when modelling swamp C flux and its controls. The set of parameters presented in the Results section will be relevant to the calibration of other temperate swamp C models. However, the high equifinality of this modelling exercise may reduce the chance of isolating specific C flux-related parameter values for modelling experiments in other temperate swamps (Sierra et al., 2015). In the event where a single parameter is selected for calibration, the parameter range of others that share the same equifinality may be affected (Wang et al., 2022; Wu et al., 2019). Also, because the selection of constraining criteria is somewhat subjective, the adoption of different sets of indices aside from R<sup>2</sup> and ME may affect the



600

605

610



outcome of the calibration and sensitivity analysis process (Metzger et al., 2016a). Therefore, caution should be taken when transferring single parameter value of Beverly Swamp to other temperate swamps. Nevertheless, the parameter ranges of the posterior distributions are applicable to the modelling of other temperate swamp systems.

## 4.3 Simulation evaluation and constraining variables for soil respiration

585 The GLUE calibration process moderately improved the performance of most simulated variables when validated with field measurements and compared to the previous results of Afolabi et al. (2025) (see Table B1 in Appendix) and prior distribution (Table 4) before multi-criteria constraint. Behavioural models of soil respiration were able to reasonably capture the seasonality of both the calibration and validation periods. However, some of the uncertainties in other simulated variables (e.g., hydrological variables) may have affected soil respiration estimates. This hypothesis was confirmed by the stepwise constraint 590 experiment on soil respiration (section 3.3) that showed that associated biophysical conditions strongly affected the acceptance or rejection rate of soil respiration simulations. LAI and hydrological variables (WTL and VMC) displayed the strongest influence on soil respiration simulations. This finding is consistent with field measurement studies that have shown that plant properties and hydrological conditions have very strong interconnections with soil respiration processes in temperate peatlands (Juszczak et al., 2013; Kendall et al., 2020; Sleeter et al., 2017). LAI is an important plant parameter in regional and global 595 biogeochemical models because it reflects important biological conditions and processes of forested ecosystems such as canopy type, canopy structure and phenological changes (Bréda, 2003; Malone et al., 2015). LAI is a major input for estimating radiation interception and energy balance (Munro et al., 2000), canopy C assimilation (Barclay, 1998), scaling between leaf resistance for water use efficiency and CO<sub>2</sub> absorption (McWilliam et al., 1993) and the simulation of evapotranspiration (Malone et al., 2015), which is an important component of water and energy balance.

Hydrological variables (saturation level, surface pool & VMC) have also been reported by many studies to have strong influence on soil respiration processes in peatlands (e.g., Davidson et al., 2019; Kendall et al., 2020; Waddington et al., 2015). Hydrological conditions moderate microbial abundance and activities, plant distribution, root growth, nutrient availability and other mechanisms that control soil respiration in wetlands (Harper et al., 2022; Mitsch et al., 1991; Nunes et al., 2015; Pezeshki, 1991). Moisture abundance partitions swamp soils into oxic and anoxic zones and this determines the rate of peat decomposition and ultimate CO<sub>2</sub> efflux into the atmosphere through soil respiration (Blodau, 2002; Limpens et al., 2008; Middleton, 2020). In particular, the evaluation of the surface pool component (Figure 5 and Table 4) was important for this experiment because of their influence on the swamp's water table level and energy flux partitioning. The underestimation of the surface pool component during the calibration and validation periods greatly reflected in the swamp's WTL and the simulation of its sensible heat flux. This mostly explained why the sensible heat flux at Beverly Swamp was poorly simulated, compared to other CoupModel studies (See Table 4), and only improved moderately for the posterior model. Consequently, the finding of this experiment will inform both modelling studies on important biophysical and biogeochemical interactions, and field measurement campaigns on the relevant variables that should be measured alongside C flux. Furthermore, the adopted





behavioural models with reduced uncertainty; high simulation performance will be an important tool for understanding future interactions and feedbacks of biophysical and biogeochemical processes in temperate swamps.

#### 615 5 Conclusion

620

625

630

640

This research is an important uncertainty modelling studies on temperate swamp peatland C dynamics, where large knowledge gaps have cumulated into substantial uncertainties in estimating the water, energy and C fluxes of this ecosystem. The adoption of the GLUE approach for uncertainty analysis assisted in achieving multiple objectives of identifying important ecohydrological processes in temperate swamp, systematically calibrating CoupModel for Beverly Swamp, improving the model performance in simulating C flux and its associated controls, and ultimately reducing the uncertainties of the modelling process. Uncertainty analysis is an important aspect of modelling experiments because it determines the usefulness of the modelling outcomes and the transferability of the modelling components (e.g., structure and parameters) to other temperate swamps. Therefore, the results of this study will inform model structure selection and parameterization of large-scale ecological models (e.g., CLASSIC and CaMP) when simulating swamp C flux at regional and global scales. Some of the important parameters and soil respiration constraining variables (e.g., WTL, VMC and LAI) that were identified in this study will help inform the choice of variables to be measured in the field for C related studies. Furthermore, the lateral flow variation experiment may also guide relevant authorities (e.g., conservation authorities) on the best approach for managing flow regulation into Beverly Swamp and similar systems towards preserving the swamp's C stocks. This is important for future planning where climate change risk may affect the hydrological and thermal conditions of the swamp, and its C balance. In addition, the behavioural models generated by the GLUE approach will be useful tools for estimating the effects of climate change on the swamp's C flux and controlling variables.

#### 5.1 Study limitations and recommendations

Although the GLUE approach assisted in reducing some of the uncertainty associated with the C flux modelling experiment at Beverly Swamp, the study is not without limitations. The rejection of all the 35,000 runs when R<sup>2</sup> and ME constraints were simultaneously applied to all the simulated variables (see section 2.4) may be an indicator of a defect in the model structure adopted for this study that does not fully capture processes relevant for temperate swamp C cycling. Therefore, there is the need for future studies to test alternative model structures that may capture better the biophysical conditions and C flux dynamics of the studied swamp, especially for the C flux and hydrological components (WTL and VMC). The uncertainty approach adopted for this study is heavily dependent on multiple variable constraints, therefore shortage of long-term field measurements for calibration and validation in some of the variables may have affected the analysis. In particular, the inclusion of high resolution multi-decadal long-term field measurements of Reco, GPP & NEE for additional variable constraint may have improved the modelling process. These measurements will help reduce the high equifinality observed for Beverly Swamp, as high equifinality can be an indication of using insufficient data for calibration (Sierra et al., 2015). Furthermore, the

https://doi.org/10.5194/egusphere-2025-1368 Preprint. Discussion started: 20 November 2025

© Author(s) 2025. CC BY 4.0 License.



645

650

655

EGUsphere Preprint repository

installation of a gauging station at the entrance of the swamp may improve the estimation of lateral influx and the effect of

Valens dam and the two creeks on the swamp. Additional measurements to support estimation of important parameters such

as growth respiration of swamp vegetation and decomposition rates of litter and humus may further reduce parameter

uncertainty in the modelling process.

The posterior parameter distribution generated from the calibration process is dependent on the variables used for constraining

the model, adopted performance thresholds, and other parameters selected for calibration. Therefore, the outcome of this

uncertainty analysis may change if these conditions are altered. Also, because the model structure selected for the simulation

of water fluxes, energy balance and C flux components in CoupModel is based on theoretical knowledge of swamp biophysical

processes and experience from existing studies, there is some level of subjectiveness in selecting the appropriate model

structure for the study (Metzger et al., 2016a; Wang et al., 2022). However, increased understanding of swamp processes and

availability of additional measurements for testing the model's structure will assist in reducing the uncertainty associated with

this modelling component.

Data availability

The version of CoupModel used to run model simulations, including the source code is hosted on Zenodo

(https://doi.org/10.5281/zenodo.16785737) and the executed CoupModel is available at www.coupmodel.com.

**Author contribution** 

660 OA and MS conducted the field design and setup, while OA led the data collection and processing. HH and OA undertook the

CoupModel setup and analysis, while OA wrote the manuscript. All the authors contributed to manuscript editing and revision.

**Competing interests** 

The authors declare that they have no conflict of interest

Acknowledgements

Hamilton Conservation Authority provided site access, while the research funding was provided by an NSERC Discovery

Grant issued to Professor Maria Strack. The location of the study site is part of the Treaty Lands and Territory of the

Mississaugas of the Credit First Nation and traditional territory of the Haudenosaunee, while the modelling work was

completed at the University of Waterloo situated on the Haldimand Tract, the land promised to the Six Nations that includes

ten kilometres on each side of the Grand River.

670

665





## References

675

685

Afolabi, O. L., Hongxing, H., & Strack, M. (2025). Process-based modelling of multi-decade carbon dynamics of a cool temperate swamp (Manuscript Submitted for Publication). *EGUsphere*, 2025, 1–44. https://doi.org/10.5194/egusphere-2024-4049

- McWilliam, A.-L. C., Roberts, J. M., Cabral, O. M. R., Leitao M. V. B. R., de Costa, A. C. L., Maitelli, G. T., & Zamparoni C. A. G. P. (1993). Leaf Area Index and Above-Ground Biomass of terra firme Rain Forest and Adjacent Clearings in Amazonia. *Functional Ecology*, 7(3), 310–317. JSTOR. https://doi.org/10.2307/2390210
- Barclay, H. J. (1998). Conversion of total leaf area to projected leaf area in lodgepole pine and Douglas-fir. *Tree Physiology*, 18(3), 185–193. https://doi.org/10.1093/treephys/18.3.185
  - Beven, K. (2006). A manifesto for the equifinality thesis. *The Model Parameter Estimation Experiment*, 320(1), 18–36. https://doi.org/10.1016/j.jhydrol.2005.07.007
  - Beven, K., & Freer, J. (2001). Equifinality, data assimilation, and uncertainty estimation in mechanistic modelling of complex environmental systems using the GLUE methodology. *Journal of Hydrology*, *249*(1), 11–29. https://doi.org/10.1016/S0022-1694(01)00421-8
- Blodau, C. (2002). Carbon cycling in peatlands—A review of processes and controls. *Environmental Reviews*, 10(2), 111–134. https://doi.org/10.1139/a02-004
- Bona, K. A., Shaw, C., Thompson, D. K., Hararuk, O., Webster, K., Zhang, G., Voicu, M., & Kurz, W. A. (2020). The Canadian model for peatlands (CaMP): A peatland carbon model for national greenhouse gas reporting. *Ecological Modelling*, 431(Journal Article), 109164. https://doi.org/10.1016/j.ecolmodel.2020.109164
  - Bréda, N. J. J. (2003). Ground-based measurements of leaf area index: A review of methods, instruments and current controversies. *Journal of Experimental Botany*, 54(392), 2403–2417. https://doi.org/10.1093/jxb/erg263
- Davidson, S. J., Dazé, E., Byun, E., Hiler, D., Kangur, M., Talbot, J., Finkelstein, S. A., & Strack, M. (2022). The unrecognized importance of carbon stocks and fluxes from swamps in Canada and the USA. *Environmental Research Letters*, 17(5),053003. https://doi.org/10.1088/1748-9326/ac63d5





- Davidson, S. J., Strack, M., Bourbonniere, R. A., & Waddington, J. M. (2019). Controls on soil carbon dioxide and methane fluxes from a peat swamp vary by hydrogeomorphic setting. *Ecohydrology*, *12*(8), e2162. https://doi.org/10.1002/eco.2162
  - Environment Canada. (2024). Climate normal. https://climate.weather.gc.ca/climate normals/
- Groemping, U. (2006). Relative Importance for Linear Regression in R: The Package relaimpo. *Journal of Statistical Software*, 710 17(1), 1–27. https://doi.org/10.18637/jss.v017.i01
  - Hamby, D. M. (1994). A review of techniques for parameter sensitivity analysis of environmental models. *Environmental Monitoring and Assessment*, 32(2), 135–154. https://doi.org/10.1007/BF00547132
- Hamilton Conservation Authority. (2020). Upper Watershed Beverly Swamp 2019 Management Plan (pp. 1–60).
  - Hanson, P. J., Edwards, N. T., Garten, C. T., & Andrews, J. A. (2000). Separating Root and Soil Microbial Contributions to Soil Respiration: A Review of Methods and Observations. *Biogeochemistry*, 48(1), 115–146. JSTOR.
- Harper, K. A., Gray, L., & Dazé Querry, N. (2022). Spatial patterns of vegetation structure and structural diversity across edges between forested wetlands and upland forest in Atlantic Canada. *Canadian Journal of Forest Research*, 51(9), 1189–1198. https://doi.org/10.1139/cjfr-2020-0247
- He, H., Jansson, P.-E., & Gärdenäs, A. I. (2021). CoupModel (v6.0): An ecosystem model for coupled phosphorus, nitrogen, and carbon dynamics evaluated against empirical data from a climatic and fertility gradient in Sweden. *Geoscientific Model Development*, 14(2), 735–761. https://doi.org/10.5194/gmd-14-735-2021
- He, H., Jansson, P.-E., Svensson, M., Meyer, A., Klemedtsson, L., & Kasimir, Å. (2016). Factors controlling Nitrous Oxide emission from a spruce forest ecosystem on drained organic soil, derived using the CoupModel. *Ecological Modelling*, 321(Journal Article), 46–63. https://doi.org/10.1016/j.ecolmodel.2015.10.030
  - Jansson, P.-E., & Moon, D. S. (2001). A coupled model of water, heat and mass transfer using object orientation to improve flexibility and functionality. *Environmental Modelling & Software*, 16(1), 37–46. https://doi.org/10.1016/S1364-8152(00)00062-1
  - Jansson, P.-K., & Karlberg, L. (2004). Coupled heat and mass transfer model for soil-plant-atmosphere systems-Coup Manual (p. 498).



740

760



Johnson, J. W. (2000). A Heuristic Method for Estimating the Relative Weight of Predictor Variables in Multiple Regression. *Multivariate Behavioral Research*, 35(1), 1–19. https://doi.org/10.1207/S15327906MBR3501\_1

- Ju, W., Chen, J. M., Black, T. A., Barr, A. G., Mccaughey, H., & Roulet, N. T. (2006). Hydrological effects on carbon cycles of Canada's forests and wetlands. *Tellus B: Chemical and Physical Meteorology*, *58*(1), 16–30. https://doi.org/10.1111/j.1600-0889.2005.00168.x
- Juszczak, R., Humphreys, E., Acosta, M., Michalak-Galczewska, M., Kayzer, D., & Olejnik, J. (2013). Ecosystem respiration in a heterogeneous temperate peatland and its sensitivity to peat temperature and water table depth. *Plant and Soil*, 366(1), 505–520. https://doi.org/10.1007/s11104-012-1441-y
- KC, U., Aryal, J., Garg, S., & Hilton, J. (2021). Global sensitivity analysis for uncertainty quantification in fire spread models.

  750 Environmental Modelling & Software, 143, 105110. https://doi.org/10.1016/j.envsoft.2021.105110
  - Kendall, R. A., Harper, K. A., Burton, D., & Hamdan, K. (2020). The role of temperate treed swamps as a carbon sink in southwestern Nova Scotial. *Canadian Journal of Forest Research*, *Journal Article*. https://doi.org/10.1139/cjfr-2019-0311
- Lavigne, M. B., & Ryan, M. G. (1997). Growth and maintenance respiration rates of aspen, black spruce and jack pine stems at northern and southern BOREAS sites. *Tree Physiology*, 17(8–9), 543–551. https://doi.org/10.1093/treephys/17.8-9.543
  - Lenhart, T., Eckhardt, K., Fohrer, N., & Frede, H.-G. (2002). Comparison of two different approaches of sensitivity analysis. *Physics and Chemistry of the Earth, Parts A/B/C*, 27(9), 645–654. https://doi.org/10.1016/S1474-7065(02)00049-9
  - Limpens, J., Berendse, F., Blodau, C., Canadell, J. G., Freeman, C., Holden, J., Roulet, N., Rydin, H., & Schaepman-Strub, G. (2008). Peatlands and the carbon cycle: From local processes to global implications a synthesis. *Biogeosciences*, *5*(5), 1475–1491. https://doi.org/10.5194/bg-5-1475-2008
- Lindeman, R. H., Merenda, P. F., & Gold, R. Z. (1980). *Introduction to Bivariate and Multivariate Analysis*. Scott, Foresman and Company.
  - Litton, C. M., Raich, J. W., & Ryan, M. G. (2007). Carbon allocation in forest ecosystems. *Global Change Biology*, 13(10), 2089–2109. https://doi.org/10.1111/j.1365-2486.2007.01420.x





- Malone, R. W., Yagow, G., Baffaut, C., Gitau, M. W., Qi, Z., Amatya, D., Parajuli, P. B., Bonta, J. V., & Green, T. R. (2015). Parameterization guidelines and considerations for hydrologic models. *Transactions of the ASABE*, 58(6), 1681–1703. https://doi.org/10.13031/trans.58.10709
- McCarter, C., Kaufman, S., Branfireun, B., & Waddington, J. (2024). Peat swamp hydrological connectivity and runoff vary by hydrogeomorphic setting: Implications for carbon storage. *Ecohydrology*, 17(3), e2637. https://doi.org/10.1002/eco.2637
  - Melton, J. R., Arora, V. K., Wisernig-Cojoc, E., Seiler, C., Fortier, M., Chan, E., & Teckentrup, L. (2020). CLASSIC v1.0: The open-source community successor to the Canadian Land Surface Scheme (CLASS) and the Canadian Terrestrial Ecosystem Model (CTEM) Part 1: Model framework and site-level performance. *Geosci. Model Dev.*, 13(6), 2825–2850.
- 780 https://doi.org/10.5194/gmd-13-2825-2020
  - Metzger, C., Jansson, P.-E., Lohila, A., Aurela, M., Eickenscheidt, T., Belelli-Marchesini, L., Dinsmore, K. J., Drewer, J., van Huissteden, J., & Drösler, M. (2015). CO2 fluxes and ecosystem dynamics at five European treeless peatlands merging data and process oriented modeling. *Biogeosciences*, 12(1), 125–146. https://doi.org/10.5194/bg-12-125-2015
  - Metzger, C., Nilsson, M. B., Peichl, M., & Jansson, P.-E. (2016a). Parameter interactions and sensitivity analysis for modelling carbon heat and water fluxes in a natural peatland, using CoupModel v5. *Geosci. Model Dev.*, 9(12), 4313–4338. https://doi.org/10.5194/gmd-9-4313-2016
- Metzger, C., Nilsson, M. B., Peichl, M., & Jansson, P.-K. (2016b). The importance of process interactions and parameter sensitivity for modelling the carbon dynamics in a natural peatland. *Geoscientific Model Development*, 1–45. https://doi.org/doi:10.5194/gmd-2016-116, 2016
- Middleton, B. A. (2020). Trends of litter decomposition and soil organic matter stocks across forested swamp environments of the southeastern US. *PLOS ONE*, 15(1), e0226998. https://doi.org/10.1371/journal.pone.0226998
  - Mitsch, W. J., Taylor, J. R., & Benson, K. B. (1991). Estimating primary productivity of forested wetland communities in different hydrologic landscapes. *Landscape Ecology*, 5(2), 75–92. https://doi.org/10.1007/BF00124662
- Muleta, M. K., & Nicklow, J. W. (2005). Sensitivity and uncertainty analysis coupled with automatic calibration for a distributed watershed model. *Journal of Hydrology*, 306(1), 127–145. https://doi.org/10.1016/j.jhydrol.2004.09.005
  - Munro, D. S. (1979). Daytime energy exchange and evaporation from a wooded swamp. *Water Resources Research*, 15(5), 1259–1265. https://doi.org/10.1029/WR015i005p01259





- Munro, D. S. (1987). Surface conductance to evaporation from a wooded swamp. *Agricultural and Forest Meteorology*, 41(3), 249–258. https://doi.org/10.1016/0168-1923(87)90081-5
- Munro, D. S. (1989). Stomatal conductances and surface conductance modelling in a mixed wetland forest. *Agricultural and Forest Meteorology*, 48(3), 235–249. https://doi.org/10.1016/0168-1923(89)90071-3

810

- Munro, D. S., Bellisario, L. M., & Verseghy, D. L. (2000). Measuring and modelling the seasonal climatic regime of a temperate wooded wetland. *Atmosphere-Ocean*, 38(1), 227–249. https://doi.org/10.1080/07055900.2000.9649647
- Nunes, F. L. D., Aquilina, L., de Ridder, J., Francez, A.-J., Quaiser, A., Caudal, J.-P., Vandenkoornhuyse, P., & Dufresne, A. (2015). Time-scales of hydrological forcing on the geochemistry and bacterial community structure of temperate peat soils. *Scientific Reports*, 5(1), 14612. https://doi.org/10.1038/srep14612
  - Ontario Government. (2019). In-filled Climate Data. https://data.ontario.ca/dataset/in-filled-climate-data/
- Jansson, P-E. (2012). CoupModel: Model Use, Calibration, and Validation. *Transactions of the ASABE*, 55(4), 1337. https://doi.org/10.13031/2013.42245
  - Pezeshki, S. R. (1991). Root responses of flood-tolerant and flood-sensitive tree species to soil redox conditions. *Trees*, *5*(3), 180–186. https://doi.org/10.1007/BF00204341

- Ryan, M. G. (1990). Growth and maintenance respiration in stems of Pinuscontorta and Piceaengelmannii. *Canadian Journal of Forest Research*, 20(1), 48–57. https://doi.org/10.1139/x90-008
- Schmidt, M., & Strack, M. (2026). Soil respiration measurements at Beverly Swamp in Southern Ontario [Dataset]. https://doi.org/10.20383/103.01050
  - Schmiege, S. C., Heskel, M., Fan, Y., & Way, D. A. (2023). It's only natural: Plant respiration in unmanaged systems. *Plant Physiology*, 192(2), 710–727. https://doi.org/10.1093/plphys/kiad167
- Sierra, C. A., Malghani, S., & Müller, M. (2015). Model structure and parameter identification of soil organic matter models. Soil Biology and Biochemistry, 90, 197–203. https://doi.org/10.1016/j.soilbio.2015.08.012



850



Silva, M. P., Healy, M. G., & Gill, L. (2024). Reviews and syntheses: A scoping review evaluating the potential application of ecohydrological models for northern peatland restoration. *Biogeosciences*, 21(13), 3143–3163. https://doi.org/10.5194/bg-21-3143-2024

Sleeter, R., Sleeter, B. M., Williams, B., Hogan, D., Hawbaker, T., & Zhu, Z. (2017). A carbon balance model for the great dismal swamp ecosystem. *Carbon Balance and Management*, 12(1), 2. https://doi.org/10.1186/s13021-017-0070-4

845 Sparks, A. H. (2018). nasapower: A NASA POWER Global Meteorology, Surface Solar Energy and Climatology Data Client for R. 3(30), 1035. https://doi.org/doi.org/10.21105/joss.01035

Sultana, Z., & Coulibaly, P. (2011). Distributed modelling of future changes in hydrological processes of Spencer Creek watershed. *Hydrological Processes*, 25(8), 1254–1270. https://doi.org/10.1002/hyp.7891

Svensson, M., Jansson, P.-E., Gustafsson, D., Kleja, D. B., Langvall, O., & Lindroth, A. (2008). Bayesian calibration of a model describing carbon, water and heat fluxes for a Swedish boreal forest stand. *Ecological Modelling*, 213(3), 331–344. https://doi.org/10.1016/j.ecolmodel.2008.01.001

Svensson, D.N., Aronsson, H., Jansson, P.-E., & Lewan, E. (2025). Insights gained from modeling grain yield, nitrate leaching, and soil nitrogen dynamics in a long-term field experiment with spring cereals on fertilized and unfertilized soil over 35 years. *Field Crops Research*, 326, 109856. https://doi.org/10.1016/j.fcr.2025.109856

Thambipillai, R. (1998). The modeling of short wave radiation transfer through the canopy of a mixed forest wetland.

860 University of Toronto.

Tonkin, J. D., Merritt, D. M., Olden, J. D., Reynolds, L. V., & Lytle, D. A. (2018). Flow regime alteration degrades ecological networks in riparian ecosystems. *Nature Ecology & Evolution*, 2(1), 86–93. https://doi.org/10.1038/s41559-017-0379-0

865 Valverde, J. (1978). Water level regimes in a swamp: Vol. MSc (p. 106). McMaster University.

Waddington, J. M., Morris, P. J., Kettridge, N., Granath, G., Thompson, D. K., & Moore, P. A. (2015). Hydrological feedbacks in northern peatlands. *Ecohydrology*, 8(1), 113–127. https://doi.org/10.1002/eco.1493

Wang, C., Li, S., Wu, M., Jansson, P.-E., Zhang, W., He, H., Xing, X., Yang, D., Huang, S., Kang, D., & He, Y. (2022). Modelling water and energy fluxes with an explicit representation of irrigation under mulch in a maize field. *Agricultural and Forest Meteorology*, 326(Journal Article), 109145. https://doi.org/10.1016/j.agrformet.2022.109145





- Welch, W. E. (1985). Structure, population processes, and successional changes of wetland forest in Beverly Swamp, Southern Ontario: Vol. MSc. York University.
  - Woo, M., & Valverde, J. (1981). Summer Streamflow and Water Level in a Midlatitude Forested Swamp. *Forest Science*, 27(1), 177–189. https://doi.org/10.1093/forestscience/27.1.177
- 880 Woo, M.-K. (1987). Hydrology of Beverly Swamp. In Steel City: Hamilton and region (Vol. 1–Book, Section, pp. 104–113).
  University of Toronto Press.
- Wu, J., Jansson, P. E., van der Linden, L., Pilegaard, K., Beier, C., & Ibrom, A. (2013). Modelling the decadal trend of ecosystem carbon fluxes demonstrates the important role of functional changes in a temperate deciduous forest. *Ecological Modelling*, 260(Journal Article), 50–61. https://doi.org/10.1016/j.ecolmodel.2013.03.015
  - Wu, M., Ran, Y., Jansson, P.-E., Chen, P., Tan, X., & Zhang, W. (2019). Global parameters sensitivity analysis of modeling water, energy and carbon exchange of an arid agricultural ecosystem. *Agricultural and Forest Meteorology*, 271, 295–306. https://doi.org/10.1016/j.agrformet.2019.03.007
  - Yang, J., Jakeman, A., Fang, G., & Chen, X. (2018). Uncertainty analysis of a semi-distributed hydrologic model based on a Gaussian Process emulator. *Environmental Modelling & Software*, 101, 289–300. https://doi.org/10.1016/j.envsoft.2017.11.037
- Yuan, F., Ricciuto, D. M., Xu, X., Roman, D. T., Lilleskov, E., Wood, J. D., Cadillo-Quiroz, H., Lafuente, A., Rengifo, J., Kolka, R., Fachin, L., Wayson, C., Hergoualc'h, K., Chimner, R. A., Frie, A., & Griffis, T. J. (2023). Evaluation and improvement of the E3SM land model for simulating energy and carbon fluxes in an Amazonian peatland. *Agricultural and Forest Meteorology*, 332(Journal Article), 109364. https://doi.org/10.1016/j.agrformet.2023.109364

900





# 905 Appendix A: Important study site properties

Table A.1 Beverly swamp site characteristics

Location and Meteorological variables	Value	Source
Lat, Lon	43.36N, 80.11W	(Munro, 1979)
Swamp size	~20 km <sup>2</sup>	(Hamilton Conservation Authority, 2020; Munro, 1979)
Altitude	265-270 m	(McCarter et al., 2024)
Mean Annual temp	7.6°C	(Environment Canada, 2024)
Mean Annual Precipitation	973 mm	(Environment Canada, 2024)
Mean Annual Evaporation	554-752 mm	(Valverde, 1978; M. Woo & Valverde, 1981)
Plant characteristics		
Major tree species (mixed forest)	silver maple (Acer saccharinum), red maple (Acer rubrum) white cedar (Cedar occidentalis), birch (Betula papyrifera), black ash (Fraxinus nigra), aspen (Populus tremuloides), elm (Ulmus americana), alder (Alnus rugosa)	(Hamilton Conservation Authority, 2020; Thambipillai, 1998; Welch, 1985)
Ground understory vegetation	Fens and Sedges	(Welch, 1985)
Average stand age in 1980	40-52 yrs	(Hamilton Conservation Authority, 2020; Welch, 1985)
Average-Max canopy height	5.22-10 m	(Hamilton Conservation Authority, 2020; Munro et al., 2000; Thambipillai, 1998)
Root depth	0.3 – 0.4 m	(Hamilton Conservation Authority, 2020; Munro et al., 2000; Thambipillai, 1998)
Leaf Area Index (LAI)	5 to 6	(Hamilton Conservation Authority, 2020; Thambipillai, 1998)
Stand density	6317-8125 trees/ha	(Hamilton Conservation Authority, 2020; Thambipillai, 1998; Welch, 1985)
Basal area	25-52 m <sup>2</sup> /ha	Welch, 1985; HCA (2021)
Average litter C/N ratio	30-93	Santia et al. (2023) & Wang et al. (2015)
Average veg C/N ratio	45.6	Wang et al. (2015)
Microbe C/N ration	6-7	Wang et al. (2015)
Plant C (1979- 1987)	$\sim 9009~gC~m^{-2}$	Welch (1985); Munro (1989); Munro et al (2000)
Foliage C	1171.17 gC m <sup>-2</sup>	Welch (1985)
Stem C	6936.93 gCm <sup>-2</sup>	Welch (1985)
Root C	900.9 gC m <sup>-2</sup> yr-1	Welch (1985)





Net Primary Productivity	~1145 gC m <sup>-2</sup> yr <sup>-1</sup>	Welch (1985)
Litter production	250-350 g m <sup>-2</sup> yr <sup>-1</sup>	Welch (1985)
Leaf longevity	0.45-8.9 years	Kanda et al (1996) & Withington et al (2006)
Phenology		
Leaf emergence day	145	Thambipillai (1998)
Leaf emergence temp	5 °C	Thambipillai (1998)
Optimum day number	167	Thambipillai (1998)
Litterfall commencement	270	Thambipillai (1998)
Canopy extinction value	0.33-0.7	Thambipillai (1998)
Soil variables		
Soil type	Sapric peat	Munro et al (2000)
peat depth	~85 (cm)	Munro et al (2000); Valverde (1978); Woo & Valverde (1981)
Soil pH	6.0 - 7.7	Spencer (1991)
Soil pore volume	80-85 vol%	Czerneda (1985); Munro (1982); Munro, 1984 & Munro et al., 2000
Soil bulk density	0.18-0.22 g cm <sup>-3</sup>	Czerneda (1985); Munro (1982); Munro (1984)
Total soil C content in upper 50 cm	$37894 \pm 14854 \text{ gC m}^{-2}$	McCarter et al. (2024)
Total soil C content in top 150	$16600 \pm 6400 \text{ gC m}^{-2}$	McCarter et al. (2024)
cm	to $106800 \pm 2800 \text{ gC m}^{-2}$	
Soil C/N ratio	18-26	DeSimone (2009); Cools et al (2014)*; Webster al at. (2014); Wang et al. (2015)
Soil nitrate	0.43-7.41 g NO <sub>3</sub> -N gsoil <sup>-1</sup>	DeSimone (2009)





# Appendix B: Additional result and charts

Table B1 Comparison of the results of initial single run and GLUE calibrated outputs

920	

Variable	Single run		This paper		
	R <sup>2</sup>	RMSE	ME	R <sup>2</sup>	ME
Soil respiration (gCm <sup>-2</sup> d <sup>1</sup> )	0.58	2.90	0.45	0.72	-0.02
SL (cm)	0.58	32.00	21.00	0.65	1.70
Snow depth (cm)	0.49	0.15	-0.21	0.52	1.00
Soil temp 5cm	0.95	2.19	1.20	0.89	3.20
Soil temp 30cm	0.92	2.02	0.46	0.92	1.60
VMC (%) 5cm	0.79	6.40	2.73	0.78	15.00
VMC (%) 30 cm	0.50	11.60	-7.71	0.52	3.00
Net radiation flux (MJ m <sup>-2</sup> d <sup>-1</sup> )	0.75	3.74	1.80	0.73	1.20
Latent heat flux (MJ m <sup>-2</sup> d <sup>-1</sup> )	0.64	2.80	0.60	0.50	-0.46
Sensible heat flux (MJ m <sup>-2</sup> d <sup>-1</sup> )	0.35	2.40	0.10	0.24	-0.12
LAI	0.80	1.00	0.61	0.74	-2.00
Surface pool (mm)	0.56	1.49	38.80	0.54	-5.40





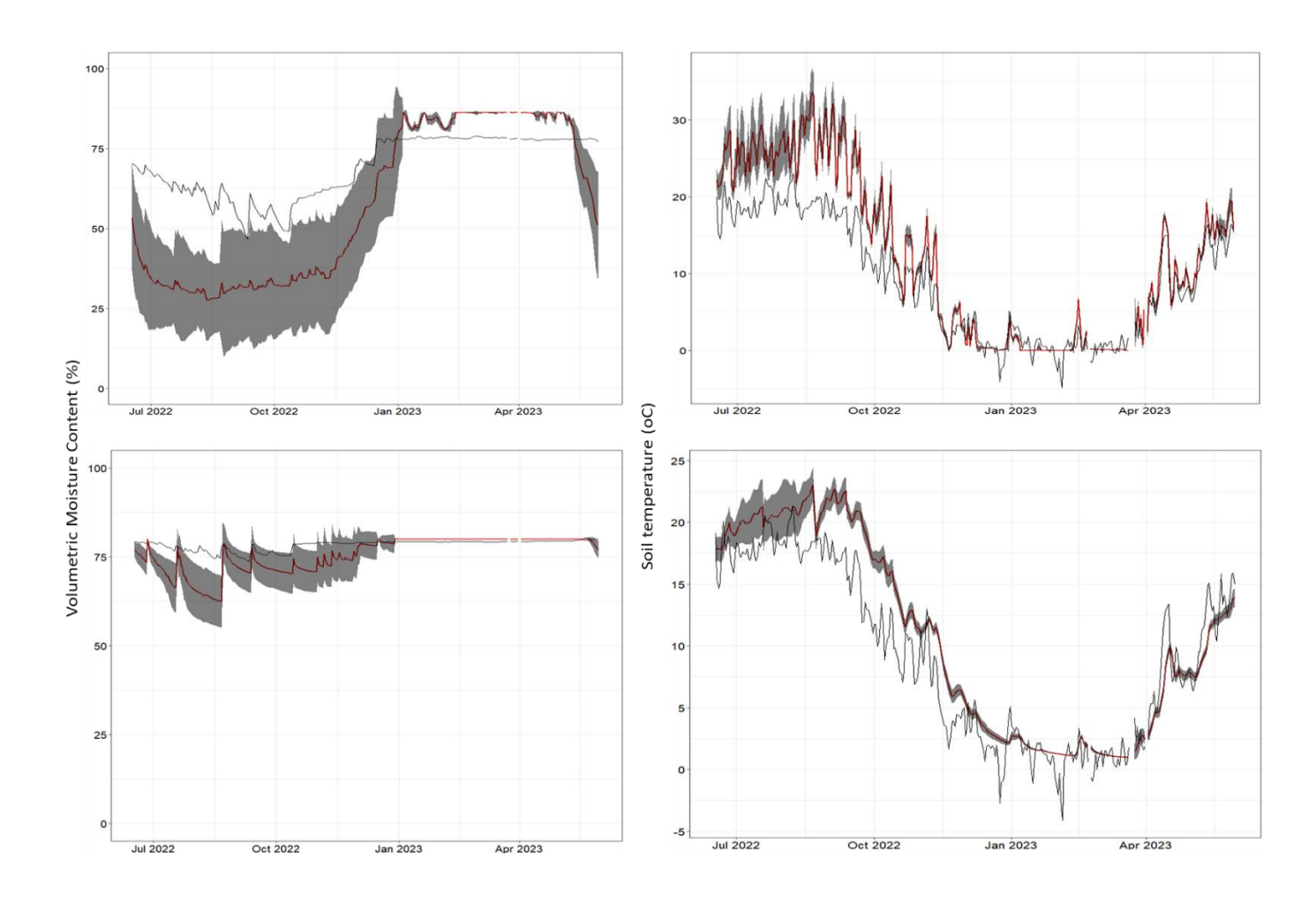


Figure B1: observation vs ensemble mean of volumetric moisture contents (5 cm & 30cm) and soil temperature simulations





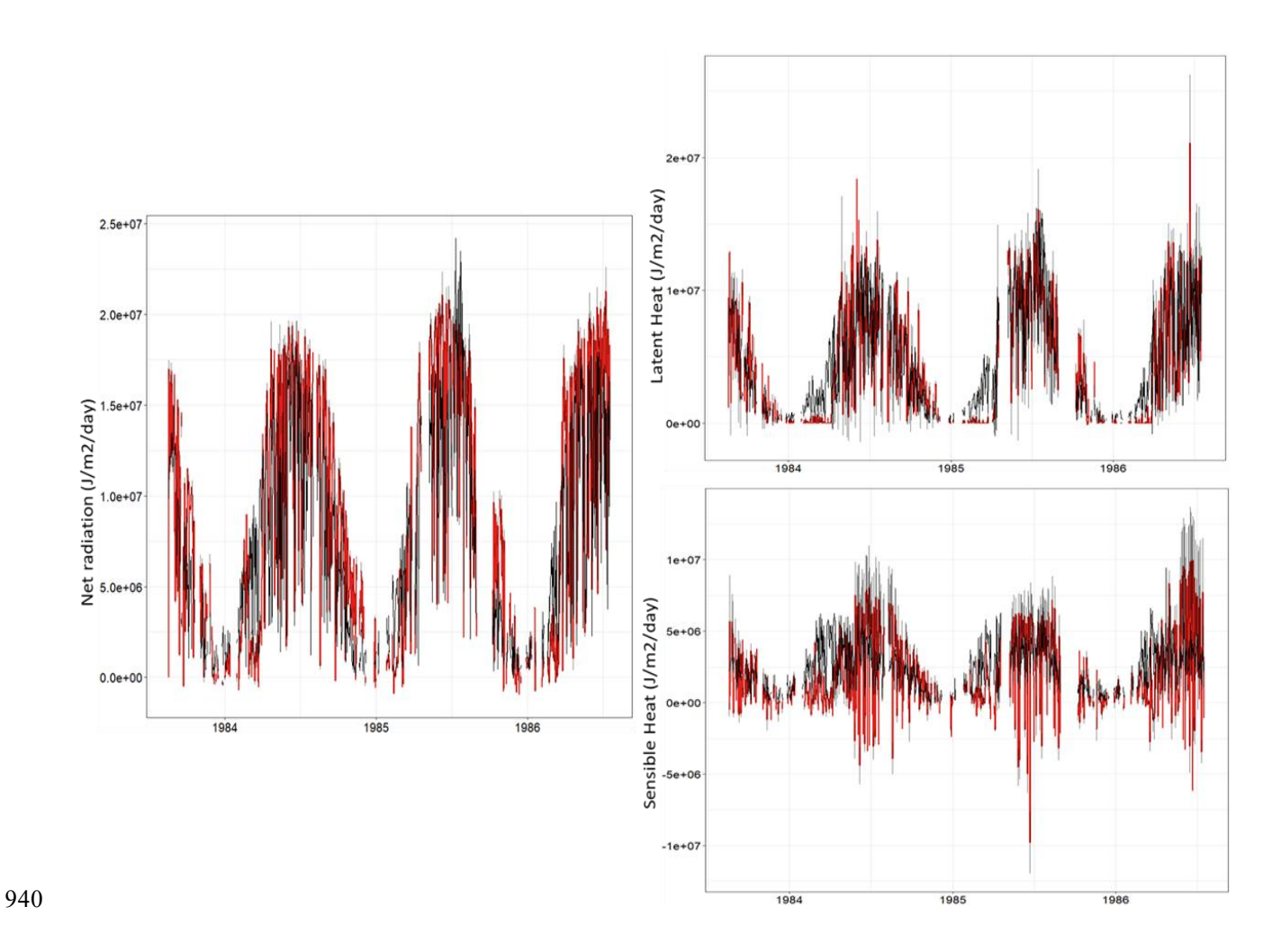


Figure B2: observation vs ensemble mean of net radiation, latent and sensible heat fluxes





R <sup>2</sup> constraint (variable)	Runs # after constraint
Soil respiration only	16,490 out of 35,000
Soil respiration + soil temperature	16,481 out of 35,000
Soil respiration + saturation level	5,923 out of 35,000
Soil respiration + WTD (saturation level and surface pool)	3,233 out of 3,5000
Soil respiration + VMC	2,678 out of 35,000
Soil respiration + VMC +WTD	1,567 out of 35,000
Soil respiration + Net radiation	16,490 out of 35,000
Soil respiration + latent heat flux	14,220 out of 35,000
Soil respiration + sensible heat flux	14,890 out of 35,000
Soil respiration + LAI	5141 out of 35000
Soil respiration + snow depth	16490 out of 35000
Soil respiration + surface pool only	6769 out of 35000

Generally, hydrological and plant productivity (LAI) variables have stronger influence than thermal variables

R <sup>2</sup> & ME (soil resp) constraint	Runs # after constraint
Soil respiration only	383 out of 35,000
Soil respiration + soil temperature	380 out of 35,000
Soil respiration + saturation level	289 out of 35,000
Soil respiration + WTD (saturation level and surface pool)	189 out of 35,000
Soil respiration + VMC	228 out of 35,000
Soil respiration + VMC +WTD	133 out of 35,000
Soil respiration + Net radiation	383 out of 35,000
Soil respiration + latent heat flux	314 out of 35,000
Soil respiration + sensible heat flux	383 out of 35,000
Soil respiration + LAI	84 out of 35,000
Soil respiration + snow depth	383 out of 35,000
Soil respiration + surface pool only	254 out of 35,000
All constraints	30 out of 35,000

Figure B3: Influence of constraining variables on soil respiration flux

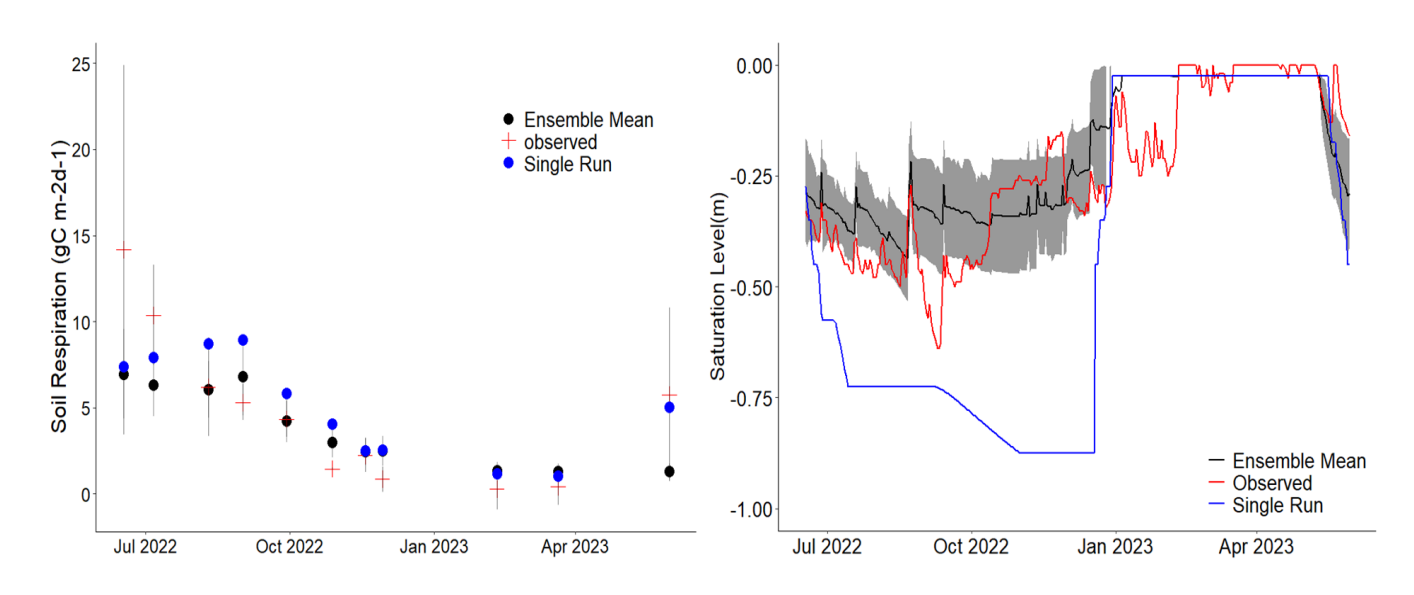


Figure B4: Results of prior single run vs GLUE result for soil respiration and saturation level